



저작자표시-비영리-변경금지 2.0 대한민국

이용자는 아래의 조건을 따르는 경우에 한하여 자유롭게

- 이 저작물을 복제, 배포, 전송, 전시, 공연 및 방송할 수 있습니다.

다음과 같은 조건을 따라야 합니다:



저작자표시. 귀하는 원저작자를 표시하여야 합니다.



비영리. 귀하는 이 저작물을 영리 목적으로 이용할 수 없습니다.



변경금지. 귀하는 이 저작물을 개작, 변형 또는 가공할 수 없습니다.

- 귀하는, 이 저작물의 재이용이나 배포의 경우, 이 저작물에 적용된 이용허락조건을 명확하게 나타내어야 합니다.
- 저작권자로부터 별도의 허가를 받으면 이러한 조건들은 적용되지 않습니다.

저작권법에 따른 이용자의 권리는 위의 내용에 의하여 영향을 받지 않습니다.

이것은 [이용허락규약\(Legal Code\)](#)을 이해하기 쉽게 요약한 것입니다.

[Disclaimer](#)

Dissertation for the Degree of Doctor of Philosophy

**A Study on the Optimization of BOG Handling for LNG-Fueled
Ship under Various Bunkering Scenarios**

Supervisor : Ho-Keun Kang

August 2019

Department of Marine System Engineering

Graduate School of Korea Maritime and Ocean University

Yude Shao

**Dissertation Submitted by Yude Shao in Partial Fulfillment
of the Requirement for the Degree of Doctor of Philosophy**

Committee Chairman : Dr. Eng. Tae-Woo Lim Ⓢ

Committee Member : Dr. Eng. Won-Ju Lee Ⓢ

Committee Member : Dr. Eng. Ki-Pyoung Kim Ⓢ

Committee Member : Dr. Eng. Yong-Seok Choi Ⓢ

Committee Member : Dr. Eng. Ho-Keun Kang Ⓢ

June 2019

Department of Marine System Engineering

Graduate School of Korea Maritime and Ocean University

Yude Shao

Contents

Contents	i
List of Tables	iv
List of Figures	v
Abstract	viii
Chapter 1 Introduction	1
1.1 Research Background	1
1.2 Dissertation Outline	5
Chapter 2 Overview of LNG Bunkering	7
2.1 LNG Bunkering Supply Chain	7
2.2 LNG Bunkering Method	9
2.3 LNG Tank and Bunkering Equipment	13
2.4 Literature Review	19
2.4.1 LNG Bunkering Technology and Safety	19
2.4.2 Current International Regulations, Standards, Class	

Rules and Guidelines	21
2.4.3 Challenges on BOG Handling	27
Chapter 3 Methodology & Process Design	30
3.1 Mathematical Model Classification	32
3.2 Dynamic Model of Main Bunkering Facilities and Equipments	38
3.2.1 LNG Tank Setup	38
3.2.2 Pipeline System Setup	45
3.2.3 Pump System Setup	49
3.3 Bunkering Process	52
3.4 Equation of State Selection & System Description ..	54
3.4.1 Equation of State Selection	54
3.4.2 System Description (STS & TTS Case)	56
3.5 Initial Conditions	57
3.6 Model Validation	60
Chapter 4 Results and Discussion	62
4.1 Disturbance of Temperature	62

4.2 Disturbance of Methane Number	69
4.3 Optimal BOG Generation in Different Bunkering Time Limits	74
4.4 Optimal BOG Generation in Different Pipe Diameter Ratio	86
Chapter 5 Conclusions	93
References	96

List of Tables

Table 2.1 Summary of various cargo-containing system for LNG	14
Table 2.2 Flexible hose for LNG bunkering	17
Table 2.3 Safety device for LNG bunkering	18
Table 2.4 Current international standards on LNG bunkering	23
Table 2.5 Summary the LNG bunkering rules of IACS members	26
Table 3.1 Geometry for the LNG tanks of bunkering and receiving ships	42
Table 3.2 Geometry for the LNG tanks of tank truck and receiving ship	44
Table 3.3 LNG mass flow rates during different bunkering time limits	51
Table 3.4 Modeling of system startup	52
Table 3.5 Modeling of system shutdown.	53
Table 3.6 Initial conditions for the STS and TTS bunkering method (Standard)	57
Table 3.7 Initial conditions for the STS bunkering method (Temperature difference)	58
Table 3.8 Initial conditions for the STS bunkering method (Methane Number)	59
Table 4.1 Quantity of state respect to different bunkering time limits (Finish Bunkering)	83

List of Figures

Fig. 1.1 World natural gas consumption	1
Fig. 1.2 MARPOL Annex VI requirements of sulfur limits (SO _x)	2
Fig. 2.1 Simplified schematic diagram of the typical LNG bunkering supply chain	8
Fig. 2.2 Standard LNG bunkering methods	9
Fig. 2.3 Trends in the LNG bunkering	12
Fig. 2.4 LNG loading arm	15
Fig. 2.5 A brief overview for the enact process in IMO for IGF and IGC Codes	22
Fig. 3.1 Simple case of a perfectly mixed tank with a single component feed for mass balance	34
Fig. 3.2 Schematic diagram of LNG pump model	49
Fig. 3.3 Simplified process flow diagram of the STS/TTS LNG bunkering scenario (Begin Bunkering)	56
Fig. 3.4 Comparison of HYSYS and Flownex simulation predicted the amount of BOG generation	61
Fig. 4.1 BOG flow rate of receiving tank	63
Fig. 4.2 Mass of BOG return from receiving tank	65
Fig. 4.3 Variations of receiving tank pressure	67
Fig. 4.4 Variations of bunkering tank pressure	67
Fig. 4.5 Total LNG bunkering amount	68

Fig. 4.6 BOG flow rate variation of receiving ship based on different MN	69
Fig. 4.7 Mass of BOG return from receiving tank	70
Fig. 4.8 Variations of receiving tank pressure	72
Fig. 4.9 Variations of bunkering tank pressure	72
Fig. 4.10 Total LNG bunkering amount	73
Fig. 4.11 BOG flow rate variation based on different bunkering time limits	75
Fig. 4.12 Effect of bunkering time on BOG generation at the receiving LNG storage tank	77
Fig. 4.13 BOG profile during bunkering operation for the BOG from the receiving tank at different bunkering time limits (50–150 min.)	77
Fig. 4.14 Pressure variation in the bunker cargo tank of the bunkering ship during the bunkering operation at different bunkering time limits	78
Fig. 4.15 Pressure variation in the fuel tank of the receiving ship during the bunkering operation at different bunkering time limits	80
Fig. 4.16 Relation between the LNG flow rate and the respective bunkering times	82
Fig. 4.17 Total bunkering amounts with respect to different bunkering times and pump stops	82

Fig. 4.18	Mass of BOG generation amount and its curve fitting result	· 84
Fig. 4.19	BOG flow rate variation based on different diameter of BOG pipeline	87
Fig. 4.20	BOG profile during bunkering operation for the BOG from the receiving tank at different diameter of BOG pipeline	89
Fig. 4.21	Pressure variation in the bunker and receiving ship during the bunkering operation at different diameter of BOG pipeline ...	90
Fig. 4.22	BOG mass and pump head during the bunkering operation at different diameter ratio of BOG and LNG pipeline	92

**A Study on the Optimization of BOG Handling for LNG-fueled Ship
under Various Bunkering Scenarios**

by Yude Shao

Department of Marine System Engineering
Graduate School of Korea Maritime and Ocean University
Busan, Republic of Korea

Abstract

Liquefied natural gas (LNG) as a marine fuel is considered as a realistic and feasible solution that complies with the stringent emissions regulation issued by International Maritime Organization (IMO). For LNG-fueled ships, the bunkering process of LNG and heavy fuel oil are completely different since the cryogenic liquid transfer generates a considerable amount of boil-off gas (BOG).

In this study, the commercial software, Aspen HYSYS V10, for process design is used to investigate and analyze the optimization in the dynamic simulation on the BOG handling between the cargo tank of a bunking ship and bunker tank of a receiving ship (LNG fueled ship) under various bunkering scenarios. With respect to the modeling of the study, for the standard ship-to-ship (STS) and truck-to-ship (TTS) LNG bunkering methods,

the diameter of the bunkering lines are set as 8 inch and 3 inch while that of the BOG return pipelines are set as 4 inch and 2 inch to satisfy the pressure of the receiving ship and BOG generation, respectively. The capacities of the cargo tank and fuel tank for bunkering and receiving ships are set as 4,538 m³ (70 m³) and 700 m³ (70 m³) for the STS and TTS LNG bunkering methods, respectively.

The results indicated that the BOG amount with different LNG bunkering scenarios is variable. The BOG flow rate varies proportionally with the temperature difference, methane number and diameter of BOG/LNG pipe in case of temperature, methane number (MN) and pipe diameter disturbance and inversely with respect to the bunkering time limit after 20 min. in case of different bunkering time limits. Additionally, for the optimal BOG handling (STS bunkering method), it is necessary to control the bunkering time within 120 min. since additional BOG is generated when the capacity of the pump exceeds 100,000 kg/h. Meanwhile, when the diameter of the BOG line (DB) divide the diameter of the LNG line (DL) $DB/DL = 0.5$ is considered the best value both in the STS and TTS LNG bunkering methods, thus the tank pressure difference between bunkering and receiving ship may be reduced.

It is believed that the results of the research could provide feasible assistance for STS and TTS LNG bunkering for the ports, and could give a specific guideline for the amount of the BOG generation and the standardized diameter of pipeline ratio.

KEY WORDS: LNG-Fueled Ship, LNG Bunkering, BOG Handling, Dynamic Simulation.

Chapter 1 Introduction

1.1 Research Background

As an alternative source of energy, the demand for liquefied natural gas (LNG) has increased rapidly. Fig. 1.1 shows that the global market for natural gas was nearly \$1 trillion in 2008. Global total natural gas consumption is expected to rise to 169 trillion cubic feet in 2035, from 111 trillion cubic feet in 2008. Natural gas consumption in emerging economies such as China and India, where consumption is forecasted to grow three times as fast from 2008 to 2035 in comparison to industrialized countries, will account for the largest part of this growth. China provides one of the largest and fastest growing opportunities, as its demand for LNG rapidly increases (IEO, 2011).

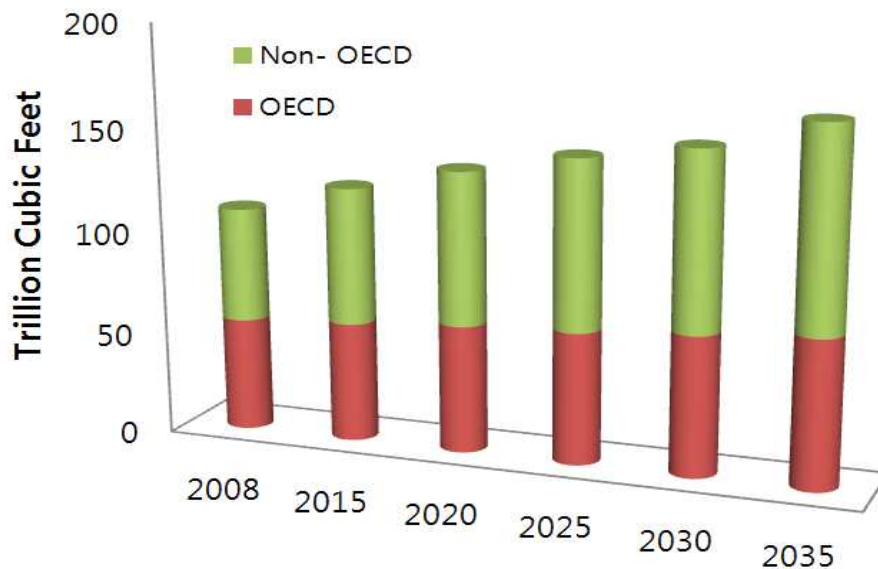


Fig. 1.1 World natural gas consumption.

In order to comply with the increasingly stringent IMO emission requirements, the use of natural gas as a ship fuel is considered as a realistic and feasible solution (Xu et al., 2015).

The schedule for the application of the stringent sulfur limits issued by International Maritime Organization (IMO) from 2015 in the emission control areas (ECAs) is in effect. The sulfur fuel emission limit which controlled by less than 0.5% will cover all over the world till 2020, as shown in Figure 1. Therefore, the current goal involves challenging ship owners and operators to determine feasible bunker for their fleet (Wang and Notteboom, 2014; Adachi et al., 2014). Three potentially feasible options include: (1) Choosing a more expensive high quality low sulfur fuel oil, such as marine gas oil (MGO), as opposed to heavy fuel oil (HFO); (2) Cleaning the exhaust gas to an acceptable emission level such as using an exhaust gas scrubber system (Notteboom, T., 2011); (3) Using the liquefied natural gas (LNG) as a fuel for ships is a realistic and feasible solution while the previous studies had indicated (Xu et al., 2015; Lee et al., 2017).

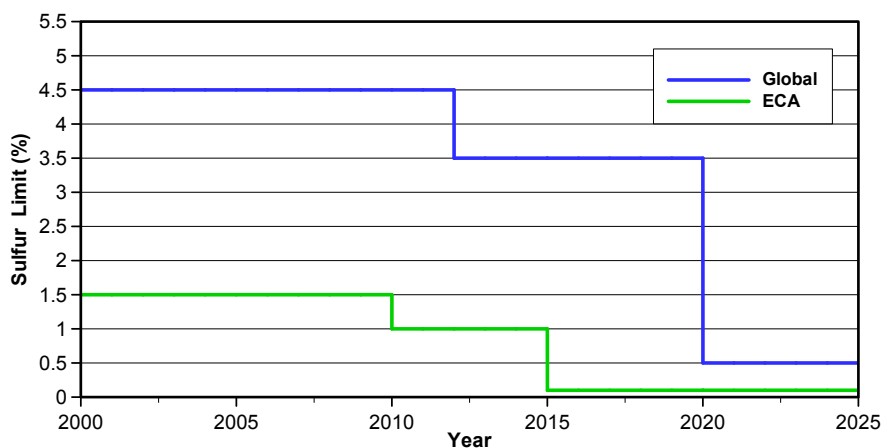


Fig. 1.2 MARPOL Annex VI requirements of sulfur limits (IMO, 2018).

Natural gas is mostly composed of methane (CH₄) which is a poisonless and flammable gas. Specifically, LNG is formed by refrigerating natural gas to a temperature below its boiling point (approximately -162 °C). The volume of the gas reduces by a factor of 600 after the liquefaction process, and thus it is widely available for transport and storage (ABS, 2014).

LNG operation, in comparison to HFO operation for ship fuel, provides a considerably cleaner exhaust, in compliance with the IMO emission regulations for gas engines operating over a broad range of power outputs. Compared with traditional marine fuel, uses LNG can reduce SO_x emissions by 90-95%, CO₂ emissions by 20-25%, and NO_x emissions by 85-90% (except the ships propelled by the ME-GI engine) (Andersen et al., 2011; Lee et al., 2015; Wang and Notteboom, 2014). Engine models include gas-only engines and dual fuel (DF) four-stroke and two-stroke engines. Dual fuel and single fuel engines have been successfully installed and operated in a number of offshore support vessels and ferry applications (Lee et al., 2017). The “Econuri,” which was the first LNG-powered vessel in Asia, was built in Korea in the 2013 and is currently operated by the Incheon Port Authority (Chun et al., 2016).

To promote the development of LNG as a ship fuel, it is necessary to set up a complete set of infrastructure facilities and to drastically improve the legal system. There are primarily three kinds of waterborne LNG bunkering methods (DNV GL, 2015): terminal-to-ship (PTS), truck-to-ship (TTS), and ship-to-ship (STS) transfers. In terms of legal provisions, the ISO/TS 18683 “Guidelines for systems and installation for supply of LNG as fuel to ships” were published in 2015. The technical specification provided guidelines for

the minimum requirements pertaining to the design and operation of an LNG bunkering facility, including the interface between LNG supply facilities, and the receipt of the ship (ISO, 2015). Moreover, one of the key steps in safe LNG bunkering is to verify that the supplying and receiving vessels are compatible. Compatibility covers a wide range of topics, and due to complexity, confirming compatibility for LNG bunkering is more important than confirming it for oil fuel bunkering.

LNG is a cryogenic liquid and its transfer can generate a significant amount of boil-off gas (BOG), and thus the LNG bunkering procedure for LNG fueled ships differs from HFO bunkering (Ryu, 2012). The BOG is caused by the heat ingress into the LNG during storage, transportation, and loading/unloading operations (Dobrata et al., 2013), and especially during the transfer of LNG fuel between the LNG supply vessel and the LNG-fueled ship while bunkering, due to temperature and pressure difference, which always results in the generation of vapor mass.

The BOG generation could cause the overpressure of the LNG tank during LNG bunkering operation. The proper treatment methods for BOG include: (a) re-liquefaction at the bunkering ship, (b) use as a fuel, and (c) burn in the flare stack (Shao et al., 2017; Yun. et al., 2015).

For ships that use LNG as a fuel, LNG bunkering is an unavoidable process. The most effective method for LNG bunkering involves transferring LNG from bunker ships to a receiving ship (LNG fueled ship) in a manner similar to the loading of LNG cargo. LNG bunkering requires paying close attention to safe operations as it entails potential risks that are directly related to cryogenic liquid transfer and BOG returns, which significantly exceeds that of the HFO bunkering.

1.2 Dissertation Outline

This dissertation dealt with the BOG generation during STS and TTS LNG bunkering process, aiming to optimize the BOG handling in various bunkering scenarios. It is organized as follows.

Chapter 2 introduced the current situation of LNG bunkering. The supply chain of LNG bunkering and the four standard bunkering methods were introduced, respectively. In addition, the LNG tank and some major bunkering equipment are highlighted.

In section 2.4, an in-depth literature review of all aspects of LNG bunkering publications provided. The last publications on technology and safety of LNG bunkering were introduced. Furthermore, a detailed survey of international rules, regulations and practices was carried in the section 2.4.2. Finally, the precedent researches focus on the BOG handling were deeply studied and analyzed in this part.

Chapter 3, theories and methods of the process simulation were presented. Firstly the linear and non-linear system were performed. Two kinds of conservation laws which are the material and component balance were highlighted.

Also, the dynamic model of the main bunkering facilities and equipments were presented in section 3.2. Then, the LNG bunkering process in this research was discussed. Next, the Peng-Robinson Equation of State and the design for the system were performed. In addition, the initial conditions for STS and TTS bunkering method in different scenarios were discussed and investigated. Finally, a model validation compared with the commercial dynamic system software Flownex was conducted. The results shown that the

gap range for the validation in each initial temperature difference was below 15%. Therefore, the simulation model we suggested was credible.

Chapter 4 presented the results of the case studies in various LNG bunkering scenarios. The disturbance of temperature and methane number was discussed firstly. Moreover, the results of optimal studies in different bunkering time limits and different pipe diameter ratios focus on the BOG generation were discussed. In addition, a mathematical model for calculating the mass of BOG generation in different bunkering time limits was developed, which was the key part of this dissertation.

Chapter 5 gave the overall conclusions and providing a reference guideline for the standard of STS and TTS LNG bunkering procedure using the optimized BOG handling techniques proposed in this dissertation. Recommendation and expectation for future application were also discussed.

Chapter 2 Overview of LNG Bunkering

The purpose of this chapter is to provide a basic overview of bunkering for LNG-fueled ships and to address the needs of a special study outlined in this dissertation. This chapter introduced the LNG bunkering supply chain, the common methods for LNG bunkering and the facilities for LNG bunkering. Therefore, after understanding the LNG bunkering profile, the reasons for BOG handling could be investigated. In addition, in the section 2.4, an in-depth literature review of all aspects of LNG bunkering publications provided a detailed survey of international rules, regulations and practices.

2.1 LNG Bunkering Supply Chain

As a typical case of LNG Bunkering Supply Chain, this section introduced in the practice in Zeebrugge port, Belgium.

Due to the proximity to the LNG import terminal and the export facilities already provided by the terminal (such as loading small LNG vessels and LNG tank trucks), the import terminal is the main potential source of supplying LNG as a marine fuel for the port.

In addition, the demand for LNG as a fuel is expected to increase dramatically, and different types of ships will need to be serviced LNG at high frequency, that will require a local storage terminal of LNG.

The intermediate storage terminal could be related to the forward distribution of LNG bunker at the port by constructing a medium-sized LNG bunker terminal (capacity: 10,000 - 40,000 m³). LNG could be delivered from the bunker terminal by installing a fixed bunkering device, bunkering ship or

truck at the bunkering terminal. The LNG supplement for the bunker terminal itself is from a large LNG import terminal by using a feeder vessel with a typical capacity of 7,500 to 30,000 m³.

The local distribution for small LNG can also occur at LNG bunkering stations using LNG tank trucks (capacity: 40~80 m³) from local bunkering terminals. As such a small scale bunkering station typically has a capacity of 100 to 3,500 m³ and are responsible for providing a limited end-user with a limited fuel consumption.

The simplified schematic diagram of the typical LNG bunkering supply chain was shown in the Fig. 2.1.

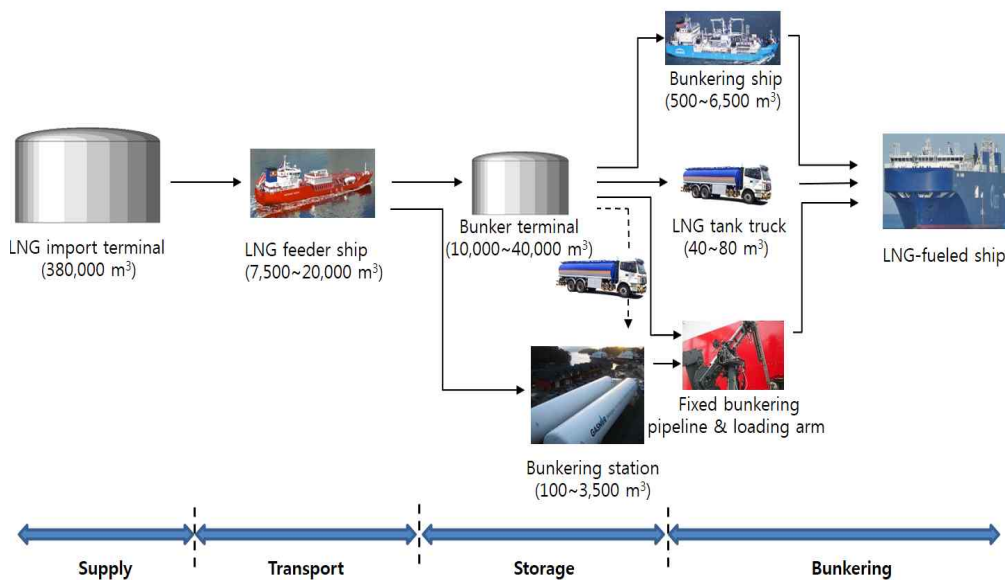


Fig. 2.1 Simplified schematic diagram of the typical LNG bunkering supply chain (based on Fluxys LNG, 2012).

2.2 LNG Bunkering Method

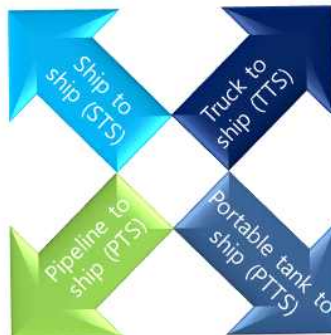
In most cases, the bunkering operation is carried out while the ship is loading and discharging cargo at the port (Jeong, 2018). For this issue, the LNG-fueled ships (except LNG carriers) have some problems because many ports currently lack LNG bunkering infrastructure (Aymelek, 2015). In order to overcome these problems, some transitional bunkering methods have been designed, as shown in Figure 2.2.



- Operational flexibility
- Large capacity
- Refilling at sea
- SIMOPS possible



- Operational flexibility
- Small investment & costs
- Possibility to adjust volumes



- Fixable
- Possibility to deliver large LNG volumes
- Good option for port with stable, long-term bunkering



- Inadequate for large ship
- Space to store tank
- Need standard size of tank
- Addition infrastructure

Fig. 2.2 Standard LNG bunkering methods (based on ISO, 2015).

1) Truck to ship (TTS) bunkering method

The TTS method is using the LNG tank truck to supply LNG to the vessel berthed in port. It is usually transported by the cryogenic flexible hose connected between the tank truck and receiving ship. For ships with small LNG fuel tanks, the TTS bunkering method can be used as an initial solution. The advantages of TTS bunkering are portable, low cost, and the ability to transport LNG over long distances. However, due to the limitation of filling speed and the capacity of tank trucks, this approach is limited for large vessels.

2) Pipeline to ship (PTS) bunkering method

In the PTS bunkering method, LNG is transferred from a fixed storage site on land through a cryogenic pipeline or hose to the LNG-fueled ship moored at a nearby dock. It can be filled not only in a large capacity, but also in portable tank. The PTS bunkering method is much faster than the TTS method and it is flexible in terms of transmission speed and capacity to meet the needs of specific customers or general customers. However, it is still a lack of geographically flexible. Because the PTS bunkering method requires the bunker station to be fixed near the LNG terminal, the ship needs to be specially arranged so that bunkering can be operated at the same time as loading and unloading to reduce the time. Otherwise, the extension of the port time will reduce the feasibility of the PTS method. However, the number of ports currently equipped with the necessary LNG bunkering facilities is very limited. As of March 2018, only 124 LNG receiving terminals were on-stream all over the world. (IGU, 2018).

3) Portable tank to ship (PTTS) bunkering method

The portable tank can be directly loaded on the ship for LNG storage. In this way, the LNG bunkering amount is very flexible, depending on the number of portable tanks. A 40-foot ISO standard intermodal tank can store approximately 40 m³ of LNG. Portable tanks can be easily transported by truck, railway and shipping. In addition, it can be stored for long periods of time (approximately 30 days by using a Type C tank). However, to use a portable tank on board, the tank and the ship must be designed with a unified standard.

4) Ship to ship (STS) bunkering method

The ship-to-ship transfer is a common bunkering practice for traditional fuel oil. Its main advantage is its high accessibility, as the LNG bunkering ship can be brought close to the receiving ship when the receiving ship is berthed. It can be used in the LNG-fueled ship in any sizes (Jeong, 2018). However, more factors need to be considered in the STS LNG bunkering process because the situation at sea is more complex than on land.

With the increase of LNG-fueled ships and the large-scale ships, the technologies and methods for adding LNG fuels are also improving. Fig. 2.3 shows the trends in the LNG bunkering. At present, the main bunkering method is that the ship was supplied LNG bunker during berthed at the dock with LNG bunkering facilities. The LNG storage tank or LNG tank truck on the land is used to supply the berthing ship with LNG through the bunkering device. The bunkering process requires the ship to occupy the pier berth or shoreline. Due to the limitation of the berths and shoreline resources of the

port, and not all ports are equipped LNG bunkering facilities. When there are more ships to be serviced, the efficiency of the ship bunkering will inevitably decrease, thus affecting the shipping efficiency of the ship. The STS LNG bunkering method has become the future development direction of LNG bunkering technology because of its self-propelled ability, safety and reliability, and flexible scheduling (Wang et al., 2018).



Fig. 2.3 Trends in the LNG bunkering (MOTIE, 2017).

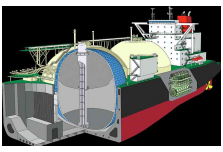
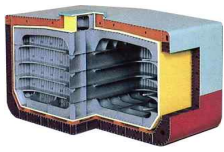
2.3 LNG Tank and Bunkering Equipment

The LNG bunkering facility refers to the physical system of terminals, storage, bunker ships, tank trucks that serve the end users to refuel. All of the LNG bunkering facilities consist the LNG tanks. Therefore, in this section, the LNG tank and some important equipment for LNG bunkering will be described.

1) LNG tank

Table 2.1 lists the characteristics and features of four types of LNG tanks that have been developed since the late 1960s. The cargo-containing system for LNG can be divided into two categories: independent and membrane. In recent years, the international research and development of A and B independent tanks and membrane tanks has been carried out. The existing LNG bunkering ships and LNG-fueled ships are mostly designed with type-C independent tanks. The LNG tank in this type has a capacity of up to 10,000 m³ by using cylindrical tanks and up to 30,000 m³ by using bilobe tanks, and a maximum allowable working pressure of 20 bar. In addition, the type C tanks are able to resist sloshing, and the polystyrene for insulation in case of the tank's capacity over 700 m³, and vacuum insulation is used for the tank's capacity less than 700 m³. Furthermore, the design of the type C tank to allow for partial loading due to it has no secondary barrier and high loading rates compared to other types (Harperscheidt, 2011).

Table 2.1 Summary of various cargo-containing system for LNG (Ikealumba and Wu, 2014; MAN, 2009; Woehrling & Cotterell, 2010; Peebles, 1992; Rudan et al., 2013).

Type	Membrane	Moss	IHI SPB	Cylindrical
Appearance	 source: GTT	 source: Kawasaki Heavy Industries	 source: IHI	 source: DNV GL
Design pressure	integrated tanks	independent Type B	independent Type B	independent Type C
Design pressure	less than 70 kPa	less than 70 kPa	less than 70 kPa	greater than 200 kPa
Capacity	145,000-265,000 m ³	145,000-265,000 m ³	145,000-265,000 m ³	145,000-265,000 m ³
Tank material	36% nickel steel (Invar) stainless steel	aluminum alloy of 9% nickel steel	aluminum alloy of 9% nickel steel	aluminum alloy of 9% nickel steel stainless steel
Insulation properties	530 mm insulation plywood boxes filled with 250-270 mm reinforced polyurethane foam	220 mm polyurethane foam	polyurethane foam	300 mm polystyrene panels
Secondary barrier	complete secondary barrier	partial secondary barrier	partial secondary barrier	no secondary barrier
Strengths/weaknesses	sloshing issue	high reliability, problems with BOG	high reliability, problems with BOG treatment	high reliability, possible to store BOG

2) LNG loading arms

Although smaller diameter 2 to 3 inch LNG hoses are easy to be operated, the larger diameters are difficult to operate. Therefore, the use of dedicated or general purpose cranes has greatly assisted in operating LNG hoses for connecting to the LNG receiving ships.

In addition, to supporting the weight of the LNG hose during bunkering, other aspects are also important drivers for the use of mechanically rigid LNG loading arms:

- i. Safety of the entire LNG bunkering operation
- ii. Accuracy of connecting/disconnecting process
- iii. Optimal bunkering duration
- iv. Possibility of supplying LNG bunker at different heights

The fully rigid arms are provided with rigid insulated pipe sections through which the LNG is pumped to the receiving ship. The swivel joint allows for the necessary movement at a predetermined degree of motion, while the pneumatic/hydraulic auxiliary mechanism provides the motion and binary force of the loading arm. The loading arm is typically installed in a fixed LNG bunkering station or an LNG-fueled ship as shown in Fig. 2.4 (EMSA, 2018).



Fig. 2.4 LNG loading arm (Carolina, 2017).

3) Flexible hose for LNG bunkering

As shown in Table 2.2, the marine LNG hoses are typically corrugated metallic type hoses (vacuum insulation) or composite multi-layer type hoses. The metallic type hose should be used with caution as the composite hose may cause the LNG remained in the fiber material and may gradually evaporate to form a flammable gas. The design, manufacturing, prototype testing and factory approval testing of the hose utilizing for LNG bunkering should in accordance with recognized standards (BS, 2008; Bas et al., 2009).

4) Safety devices for LNG bunkering

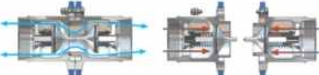
The “Emergency Shut Down system” (ESD) is the most critical system in the LNG bunkering safety system. The primary purpose of the ESD system is to shut down the source of ignition to reduce the risk of explosions in case of a gas leakage during bunkering process (SMTF, 2010). In addition, some of the major components in the ESD system were listed in Table 2.3.

According to the classification of LNG terminal operations, the ESD system is divided into two levels, namely ESD-I and ESD-II. The ESD-I is the interrupted LNG transmission, and ESD-II is the complete separation (including mooring lines) between the pier and the ship. A two-stage ESD system can also be considered for LNG bunkering operation. After the ESD-I is started, the LNG bunkering pump and the pressure build-up device of tank should be automatically shut down. The hot-state and cold-state test of the ESD system should be carried out before LNG bunkering (Xu et al., 2015).

Table 2.2 Flexible hose for LNG bunkering (EMSA, 2018).

Equipment	Description	Type	Remarks
Hose	For LNG transfer and vapor return service	<ul style="list-style-type: none"> • Metallic type  <ul style="list-style-type: none"> • Composite multi-layer type 	<ul style="list-style-type: none"> • Suitable for small bunkering capacity via LNG truck • Suitable for large bunkering capacity via STS bunkering
Hose Saddle	For providing critical support for the hose assembles whilst maintaining the correct hose form.	<ul style="list-style-type: none"> • Fixed height type  <ul style="list-style-type: none"> • Adjustable height type 	<ul style="list-style-type: none"> • Marine grade aluminum construction • Possible for multi-hose routes • Possible for integral fall arrest system (FAS)

Table 2.3 Safety device for LNG bunkering (ERC, BRC, QCDC) (EMSA, 2018).

Equipment	Description	Type	Remarks
<p>ERC (Emergency Release Coupling)</p> <p>BRC (Breakaway Release Coupling)</p>	<p>Safety coupling located in LNG transfer system which separates at the predetermined section at the determined break load or the relative separation distance, each of separated section including a self-closing shut-off valve, which automatically seals</p>	<ul style="list-style-type: none"> • Flip-flap type  • Spring loaded type  	<ul style="list-style-type: none"> • Powered by hydraulic stem for release mechanism • Powered by HP N₂ system for release mechanism
<p>QCDC (Quick Connect/ Disconnect Coupling)</p>	<p>For quick and spill free connection and disconnection of hoses and pipelines</p>	<ul style="list-style-type: none"> • Hydraulically operated type  • Manual type  	<ul style="list-style-type: none"> • Suitable for marine loading arm • Suitable for LNG hose transfer system

2.4 Literature Review

2.4.1 LNG Bunkering Technology and Safety

For ships that use LNG as a fuel, LNG bunkering is an unavoidable process. The most effective method for LNG bunkering involves transferring LNG from bunker ships to a receiving ship (LNG-fueled ship) in a manner similar to the loading of LNG cargo. LNG bunkering requires paying close attention to safe operations as it entails potential risks that are directly related to cryogenic liquid transfer and BOG returns, which significantly exceeds that of the HFO bunkering. Therefore, extant studies focused on the bunkering procedure or the safety of using LNG as a marine fuel.

Wang and Notteboom (2015) carried out a multi-case study method to analyze the performance of eight North European port authorities in the LNG bunkering projects. Analyzed the port authority's role in the development of LNG bunkering facilities and the investigation into how and why the port authority is promoting this new application.

Lee et al. (2016) conducted a study based on the technical feasibility of both the LNG storage tanks and the BOG treatment systems in the LNG ship-to-ship bunkering chain. And the three major ports with high potential for LNG bunkering were selected as case studies to verify the validity of the

model.

Yun et al. (2015) examined a conceptual design of an offshore liquefied natural gas (LNG) bunkering terminal for Busan port in Korea. As a case study, they performed a conceptual design by analyzing the statistics of visiting ships, estimating the required LNG consumption, and determining the process specifications and equipment features.

Fan et al. (2017) using the CFD software FLACS to investigate the safety zone during the STS LNG bunkering process with a 10,000 m³ capacity LNG bunkering ship and a 18,000 TEU container ship. By calculating the diffusion of flammable clouds dispersion after LNG leakage. A rectangular dangerous zone (41.3 m × 126 m) was obtained, which the safety zone can be defined as the outside of the dangerous zone.

Sun et al. (2017) conducted a numerical analysis of hazardous consequence during ship-to-ship LNG bunkering that could involve the LNG vapor dispersion and LNG pool fires. They used computational fluid dynamics (CFD) models to qualitatively and quantitatively examine the main characteristics of different hazard types, vapor dispersion, and fire radiation.

Jeong et al. (2017) using integrated quantitative risk assessment (IQRA), proposed a statistical method to determine the safe exclusion zone around the LNG bunkering station and identify the potential risks during LNG bunkering.

2.4.2 Current International Regulations, Standards, Class Rules and Guidelines

1) International regulations and standards

IMO regulations

The International Maritime Organization (IMO) has developed two international Codes on the LNG carriers and LNG-fueled ships : *International Code of the Construction and Equipment of Ships Carrying Liquefied Gases in Bulk* (IGC Code), in 1986 and subsequent amendments in 1994 and 2014 and *International Code of Safety for Ship Using Gases or Other Low-flashpoint Fuels* (IGF Code), which came into force on 01 January 2017 (Ha et al., 2019).

Fig. 2.5 expressed a conceptual diagram that provides a brief overview for the enactment process of the two Codes in IMO.

Moreover, to ensure that using LNG as a marine fuel is the safety and feasible alternative, the regulations for the bunkering process must be consistent. Although the draft IGF specification deals with bunkering issues to a certain extent, the main focus is on the LNG-fueled vessels. It is worth noting that the comprehensive operational guidance on the interface between the bunker ship and the receiving ship is seriously inadequate (Xu et al., 2015).

In this regard, the shortages of the draft in IGF Code with the interface between the bunkering facility and the receiving ship are highlighted in the ISO / TS 18683 : 2015 standard published by the International Organization for Standardization (ISO). Other ISO standards were discussed in the next section.

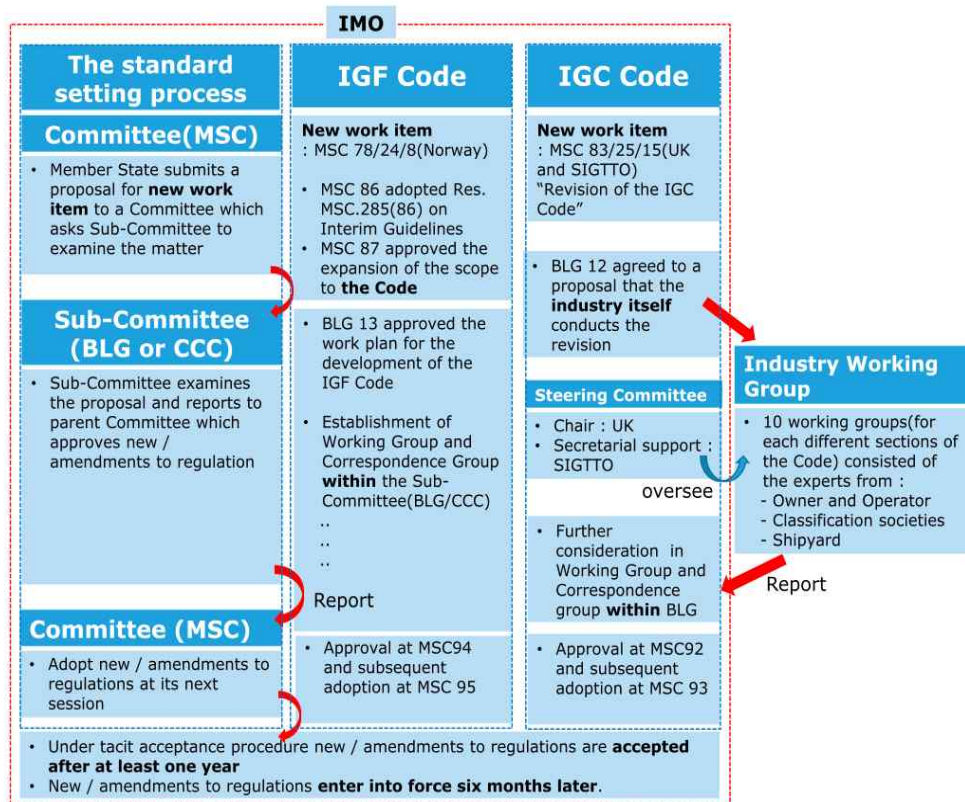


Fig. 2.5 A brief overview for the enact process in IMO for IGF and IGC Codes (Ha et al., 2019).

ISO standards

The International Organization for Standardization (ISO) is a non-governmental organization composed of representatives of a number of major member national standardization organizations. It has published various standards on LNG terminals, LNG carriers and LNG bunkering equipments. Current standards on LNG bunkering were listed in Table 2.4.

Table 2.4 Current international standards on LNG bunkering (ISO, 2008~2017).

Standard No.	Title
ISO 20519:2017	Ships and marine technology — Specification for bunkering of liquefied natural gas fuelled vessels
ISO/TS 18683:2015	Guidelines for systems and installations for supply of LNG as fuel to ships
ISO 19970:2017	Refrigerated hydrocarbon and non-petroleum based liquefied gaseous fuels — Metering of gas as fuel on LNG carriers during cargo transfer operations
ISO 16924:2016	Natural gas fuelling stations — LNG stations for fuelling vehicles
ISO 16904:2016	Petroleum and natural gas industries — Design and testing of LNG marine transfer arms for conventional onshore terminals
ISO/TS 16901:2015	Guidance on performing risk assessment in the design of onshore LNG installations including the ship/shore interface
ISO 10976:2015	Refrigerated light hydrocarbon fluids — Measurement of cargoes on board LNG carriers
ISO/TR 17177:2015	Petroleum and natural gas industries — Guidelines for the marine interfaces of hybrid LNG terminals

Standard No.	Title
ISO 18139:2017	Ships and marine technology — Globe valves for use in low temperature applications — Design and testing requirements
ISO 12614-2:2014	Road vehicles — Liquefied natural gas (LNG) fuel system components — Part 2: Performance and general test methods
ISO 15500-19:2012	Road vehicles — Compressed natural gas (CNG) fuel system components — Part 19: Fittings
ISO 8310:2012	Refrigerated hydrocarbon and non-petroleum based liquefied gaseous fuels — General requirements for automatic tank thermometers on board marine carriers and floating storage
ISO 13706:2011	Petroleum, petrochemical and natural gas industries — Air-cooled heat exchangers
ISO 28460:2010	Petroleum and natural gas industries — Installation and equipment for liquefied natural gas — Ship-to-shore interface and port operations
ISO 19906:2010	Petroleum and natural gas industries — Arctic offshore structures
ISO 13709:2009	Centrifugal pumps for petroleum, petrochemical and natural gas industries
ISO 18132-2:2008	Refrigerated light hydrocarbon fluids — General requirements for automatic level gauges — Part 2: Gauges in refrigerated-type shore tanks

2) Class rules and guidelines

A number of classification societies have established rules for the use of LNG as a marine fuel and LNG bunkering operation, which are to varying degrees based on the 2009 *Interim Guidelines for Natural Gas Fuel Vessels* and the draft IGF Code (Xu et al., 2015).

The purpose of the classification society is to provide certification, legal services, support to the maritime industry and inspection agencies. The International Association Classification Society (IACS) was established in 1968, following the cooperation among the classification societies specified in the *International Load Line Convention*. Currently, it is composed of 12 class members including Korean Register of Shipping (KR) and China Classification Society (CCS).

In most cases, the classification society developed the guidelines for the marine liquified natural gas bunkering for ships based on the *Interim Guidelines on Safety for Natural Gas-Fuelled Engine Installations in Ships MSC.285(86)*. In MSC.285 (86), this class rule provides guidance on the design, construction and operation of natural gas fuelled vessels and is not legally binding. Consequently, each flag state must agree to operate a gas fuelled vessel that sails on the national waterways. Currently, the above class rules are used for the permission process.

Table 2.5 summarized the LNG bunkering rules and guidelines of IACS members based on *Interim Guidance MSC.285 (86)* (GL, 2013).

Table 2.5 Summary the LNG bunkering rules of IACS members (GL, 2013).

No.	Name of Class	Class short sign	Title of Guideline
1	International Association Classification Society	IACS	IACS Rec 142 LNG Bunkering Guidelines (2016)
2	American Bureau of Shipping	ABS	LNG Bunkering Technical and Operational Advisory (2014)
3	Bureau Veritas	BV	Guidelines on LNG bunkering(2014)
4	China Classification Society	CCS	Guidelines for LNG Fuel Bunkering Operation (2017)
5	Croatian Register of Shipping	CRS	-
6	Det Norske Veritas & Germanischer Lloyd	DNVGL	P-G105 Development and operation of liquefied natural gas bunkering facilities (2015)
7	Indian Register of Shipping	IRCLASS	-
8	Korean Register of Shipping	KR	Guidelines for Floating LNG Bunkering Terminal (2018)
9	Lloyds Register	LR	Rules and regulations for the classification of natural gas-fuelled ships (2012)
10	Nippon Kaiji Kyokai	NK	Guidelines for the issuance of ship fuel gas (2012)
11	Polish Register of Shipping	PRS	Guidelines on safety for natural gas-fuelled engine installations in ships; publication No. 88/P (2012)
12	Italian Register	RINA	Rules for the classification of ships, Amendments to part C, Chapter 1: New Appendix 7 – Gas-fuelled ships (2011)
13	Russian Maritime Register of Shipping	RS	-

2.4.3 Challenges on BOG Handling

For the challenges on BOG handling, various studies have been done on the behavior of the BOG generation at the LNG exporting terminals, the LNG-FPSO and during transportation by utilizing Aspen simulation software and the Computational Fluid Dynamics (CFD) technology.

Kurle et al. (2015) proposed several BOG recovery strategies and using steady-state simulations for BOG generation at LNG exporting terminals using Aspen Plus software. They found that the temperature of liquefied natural gas (LNG) had a significant effect on BOG generation, and concluded that the subcooling LNG could reduce the BOG generation.

In 2016, Kurle et al. (2017) also conducted effects of the temperature of LNG ship-tank, the jetty boil-off gas (JBOG) compressor capacity and the rate of tank cooling on JBOG generation utilizing Aspen Dynamics simulation.

Kurle et al. (2018) utilized dynamic simulation to quantify the amount of boil-off gas generated from LNG plants/terminals in different operating modes. The authors recommended to sub-cool the LNG after the main cryogenic heat exchanger to reduce the occurrence the boil-off gas and determine the optimum temperature for LNG that minimizes total energy consumption.

Hasan et al. (2009) worked on the minimizing boil-off during LNG transportation using the Soave-Redlich-Kwong (SRK) state property equation

method to conduct a dynamic simulation of LNG transportation process in Aspen HYSYS process simulation software. As a result, they identified various key and effective factors for BOG generation, such as the tank pressure, ambient temperature, cruise range and nitrogen content.

Yan and Gu (2010) performed the a full scale model to analyze the effect of the BOG generation, the mass flow rate and the pump head of the LNG offloading system during LNG transfer process from the floating production storage and offloading unit for liquefied natural gas (LNG-FPSO) to the LNG carrier with the Aspen Plus software.

Zakaria et al. (2014) carried out the a study by using the realistic parameters and assumptions to analyze the calculation of boil-off gas rate for large scale LNG tanks. The ANSYS Fluent software was used to analyze both the steady and transient behavior of heat transfer mechanisms.

Migliore et al. (2015) presented an LNG vapor-liquid equilibrium model for LNG storage on shore. According to their research results, it was reported that for every 1°C change in ambient temperature, the BOG changes by 0.2%.

Miana et al. (2010) presented two different models involving BOR for calculating the phenomenon of LNG ageing during ship transportation.

In 2016, Miana et al. (2016) utilized the numerical analysis to calculate the BOG generation rate of cargo tanks on LNG carriers. The heat flow models were compared to predict evaporation rate of LNG during shipping.

Sharafian et al. (2016) analyzed the performance of LNG storage tanks in refueling stations. Based on the results of their research, the ratio of heat transfer surface area to liquefied natural gas volume is a key factor in comparing the holding times of the storage tanks in different sizes.

Bahgat, M.W. (2015) provided an overview of current method of natural gas transportation and a method for saving BOG amount. The method is in a 266,000 m³ size LNG carrier, the BOG could be treated in two PLNG containers.

Park et al. (2012) conducted a concept retrofit design for a boil-off gas handling process in the liquefied natural gas receiving terminals using a fundamental analysis. Aspen process simulation was adopted and the Sequential Quadratic Programming (SQP) solver in MATLAB was used to optimize the values of design variables.

Rao et al. (2018) developed a novel type of superstructure for BOG re-liquefaction including all process options, and for a case study, the optimal configuration of BOG re-liquefaction corresponding to different amount of BOG in the LNG re-gasification terminal.

Chapter 3 Methodology & Process Design

“General Purpose Chemical Process Simulation” refers to the use of thermodynamics to model the chemical engineering in mathematics, which is defined as the software to simulate the actual situation of oil refining and petrochemical plants by computer. It is also known as the *process flow sheet*.

Westerberg et al. (1979) also defined flow sheet as the use of computer aids to perform steady-state heat and mass balancing, sizing, and costing calculations for a chemical process.

The biggest advantage of the chemical engineering simulator is that as long as the physical property value, flow rate and operating conditions of the object actually put into the project are input, the results can be almost the same as the actual situation with very little time and cost even if the chemical plant is not actually started.

Most of the description of the chemical engineering can show the Differential Algebraic Equations (DAEs), in order to describe in detail, can be extended to include the general variable Integral Partial Differential equation of Integral Partial Differential Equations (IPDEs). The number of equations used in chemical engineering ranges from thousands to tens of thousands. It can be broadly divided into two categories : (i) Sequential Modular Method and (ii) Equal-Oriented Method.

Most of the existing molds adopt the sequential module method. However, recently with the improvement of computer technology, the equal-oriented method is utilized. Even with the equal-oriented method, the recent trend is towards a mixture of the sequential module method. The sequential module

method is included as a subprogram or computation process independent of the unit and the thermodynamic modeling. On the other hand, the equation-oriented method is that the process equations are gathered together and calculated at the same time. In the case of the equation-oriented method solver, the function of dealing with the sparse matrix, which is common in the modeling of chemical processes, must be excellent and the convergence speed of the solution must be fast. Simulators based on Sequential Modular Method include Aspen Plus, Aspen HYSYS, PRO/II, etc. while the simulators based on Equal-Oriented Method include SPEEDUP, gPROMS, etc. In this study, Aspen HYSYS is used which contains a database with approximately 1,700 pure elements. Besides, it also has built-in modules that can simulate 60 thermodynamic model equations and approximately 70 unit operation devices (Aspen, 2017).

3.1 Mathematical Model Classification

In a real process, physical changes have directionality with respect to x, y, and z axes over time and can be mathematically defined through Partial Differential Equations (PDEs) in general. If orientation is not taken into account, it is considered as a Lumped Model, and all properties are considered the same in the same system. In other words, in a unit or hold up volume, it is assumed that a three-dimensional equation is not used, and only a time gradient is considered in the analysis. These conditions can be accounted for by much less stringent ordinary differential equations than partial differential equations and can shorten the computation time.

Aspen HYSYS uses a lumped model and does not consider thermodynamic or concentration gradients in a single phase. In other words, it is assumed that the temperature and composition in each phase are all the same (Aspen, 2017).

3.1.1 Linear & Non-Linear Systems

A linear First-Order ODE is expressed as follows:

$$\tau \frac{dY}{dt} + Y = Kf(u) \quad (3.1)$$

In the nonlinear differential equation, the Y variable means exponential function or other system and independent variable, and can be expressed as Equations 3.2 and 3.3.

$$\tau \frac{dY}{dt} + Y^3 = Kf(u) \quad (3.2)$$

$$\tau \frac{dY}{dt} + Y Y_2 = Kf(u) \quad (3.3)$$

Most of the chemical processes that occur in general are nonlinear. This nonlinearity is caused by the equilibrium, the fluidity of the fluid, or the reaction rate of the chemical system. For this reason, the general linear system equations can be solved analytically through matrix algebra, but the solution to the nonlinear equations can be found by computer operation.

3.1.2 Conservation Laws

1) Mass Balance

In Aspen HYSYS, the mutual conservation of material is based on mathematical modeling. In dynamic model, the flow, component, and energy balances are expressed in a similar way to the material balances, except for the accumulation term in the steady model. The accumulation term is because the system exhibits various results over time.

In general, the flowrate conservation is expressed as Equation 3.4.

$$\begin{aligned} \text{Rate of accumulation of mass} &= \text{mass flow into system} \\ &- \text{mass flow out of system} \end{aligned} \quad (3.4)$$

The flow reserve of a tank containing a single substance is shown in Fig. 3.1.

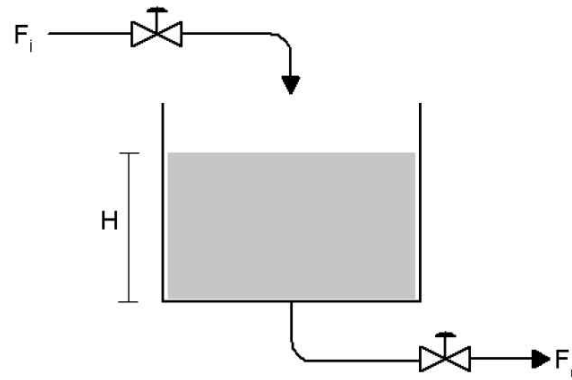


Fig. 3.1 Simple case of a perfectly mixed tank with a single component feed for mass balance (Aspen, 2017).

Equation 3.5 simply expressed the equation considering complex properties such as phase change, reaction rate, and density change in Aspen HYSYS. Actual process modeling takes into account various physical properties and conservation of physical quantities.

$$\frac{d(\rho_o V)}{dt} = F_i \rho_i - F_o \rho_o \quad (3.5)$$

where:

V = Tank Volume

F_i = Flow of Component into System

ρ_i = Fluid Density into System

F_o = Flow of Component out of System

ρ_o = Fluid Density out of System

2) Component Balance

The component balance can be expressed as Equation 3.6 (Aspen, 2017).

$$\begin{aligned} \text{Rate of accumulation of component } j &= \text{Flow of component } j \text{ into system} \\ &\quad - \text{Flow of component } j \text{ out of system} \\ &\quad + \text{Rate of formation of component } j \text{ by reaction} \end{aligned} \quad (3.6)$$

The flow rate into and out of the system is convective or diffusive. If both the surface system and the volume ratio are high in the particulate phase, the convective flow is due to the major outflow flow into the system, resulting in a considerable convective flow.

The balance of the polyphase fluid phase composition in a perfectly mixed tank can be defined as Equation 3.7.

$$\frac{d(C_{jo} V)}{dt} = F_i C_{ji} - F_o C_{jo} + R_j V \quad (3.7)$$

where:

C_{ji} = Flow of component j into system (Multiphase)

C_{jo} = Flow of component j out of system (Multiphase)

R_j = Reaction rate of component j

3) Energy Balance

The energy balance is defined by Equation 3.8 (Aspen, 2017).

$$\begin{aligned} \text{Rate of accumulation of total energy} &= \text{Flow of total energy into system} \\ &\quad - \text{Flow of total energy out of system} \\ &\quad + \text{Heat added to system across its boundary} \\ &\quad + \text{Heat generated by reaction} \\ &\quad - \text{Work done by system on surroundings} \end{aligned} \quad (3.8)$$

The energy flow into and out of the system is exchanged by convection or conduction. The incoming heat from the external system is transferred by conduction or radiation.

The typical energy balance of the Continuous Stirred-Tank Reactor (CSTR) is shown in Equation 3.9.

$$\frac{d}{dt} [(u + k + \Phi) V] = F_i \rho_i (u_i + k_i + \Phi_i) - F_o \rho_o (u_o + k_o + \Phi_o) + Q + Q_r - (w + F_o P_o - F_i P_i) \quad (3.9)$$

where:

u = Internal energy (energy per unit mass)

k = Kinetic energy (energy per unit mass)

Φ = Potential energy (energy per unit mass)

V = Volume of the fluid

w = Shaft work done by system (energy per time)

P_o = Vessel pressure

P_i = Pressure of feed stream

Q = Heat added across boundary

Q_r = Heat generated by reaction

To simplify the expression, some of the following assumptions can be applied (Aspen, 2017).

i) Potential energy is mostly negligible. That is, the inlet and outlet gradients are the same.

ii) If the inlet and outlet flow velocities are not high, ignore kinetic energy terms.

iii) If there is no shaft work, that is, if there is no rotating device like pump, $w = 0$.

Considering these assumptions, the general energy balance of a two-phase system is given by Equation 3.10.

$$\frac{d}{dt}[\rho_v V_v H + \rho_l V_l h] = F_i \rho_i h_i - F_l \rho_l h - F_v \rho_v H + Q + Q_r \quad (3.10)$$

3.2 Dynamic Model of Main Bunkering Component and Facility

The main component and facility for the LNG bunkering process are mainly include the LNG tank, pipeline and pump. The dynamic models of the main component and facility are described in the following sections.

3.2.1 LNG Tank Setup

1) Theoretical method

During the LNG bunkering process, it is inevitable that the BOG is flashed in the LNG receiving ship, and the BOG is returned to the LNG bunkering ship via the BOG return pipeline.

To simplify the LNG fuel tank model, the momentum change is ignored, and only the time gradient is considered. The overall energy conservation equations and the mass conservation equations of the vapor and liquid phases described by the ordinary differential equation are as follows:

Mass Conservation Equation (Liquid)

$$\frac{d(V_L \rho_L)}{dt} = M_L - M_{EVA} \quad (3.11)$$

where:

V_L = Liquid volume

ρ_L = Liquid density

M_L = LNG mass flow at the inlet of the tank

M_{EVA} = Gas mass of vaporized liquid

Mass Conservation Equation (Vapor)

$$\frac{d(V_V \rho_V)}{dt} = M_{EVA} - M_V \quad (3.12)$$

where:

ρ_V = Vapor density

M_V = BOG mass flow at outlet of the tank

Energy Conservation Equation

$$\frac{d(V \rho h_L)}{dt} = M_L h_L + Q + Q_{EVA} - M_V h_V \quad (3.13)$$

where:

Q = Heat loss from the tank to the fluid

Q_{EVA} = Fluid-oriented heat flow at the gas-liquid boundary

h_L = Enthalpy value of the liquid

h_V = BOG enthalpy value at tank outlet

2) Heat ingress

For the LNG tanks in each case, the vapor and the liquid in the tank are assumed to be in thermal equilibrium. The heat ingress through the walls of the LNG fuel tank depends on the temperature of ambient. Since the heat transfer from the ambient to the LNG fuel tank is a combination of conduction and convection, the Q can be expressed as Equation 3.10 (Migliore 2015).

$$Q = U \cdot A \cdot \Delta T = (U_L A_L + U_V A_V) \cdot (T_A - T) \quad (3.14)$$

where:

U = Overall heat transfer coefficient

A = Contact area

U_L = Overall heat transfer coefficient of liquid phase

U_V = Overall heat transfer coefficient of vapor phase

A_L = Contact area of liquid phase

A_V = Contact area of vapor phase

T_A = Ambient temperature

T = Temperature at thermal equilibrium in tank

3) Tank bunkering/filing limit and tank heel

Generally, the bunkering limit denotes the maximum allowable liquid volume to which the fuel tank may be loaded, and which is expressed as the percentage of the total fuel tank volume. The limit depends on the LNG densities at the bunkering and reference temperatures and is determined as follows:

$$BL = FL \left(\frac{\rho_R}{\rho_L} \right) \quad (3.15)$$

Here, BL denotes the bunkering limit, FL denotes the tank filling limit, and subscripts ρ_R and ρ_L denote the LNG density at reference temperature and the LNG density at bunkering temperature, respectively. If the LNG tank is the pressure-vessel type, it could sustain a pressure as 10 barg. So that the typical bunkering limits for the LNG-fueled ships are expected to range from 85% to 95% based on the fuel tank type, pressure relief valve setting, and

other ship specific considerations (ISO, 2017). Therefore, in the study, the bunkering time limit for each case is set to the level reached by the LNG fuel tank of the receiving ship at 90%.

The LNG bunkering can be operated only after the LNG fuel tank is inert, purged, and cooled down. With respect to the beginning of the simulation, the cool down process is only considered to accomplish using cold natural gas or LNG.

During transfer, the ship's fuel tanks typically contain an amount of LNG. In general, the volume remaining in the tank before bunkering is called heel, this small quantity is necessary to keep the tank cold prior to bunkering. The required tank heel in receiving ship is normally calculated by the fuel gas designers and the tank designers according to several variables (tank size, ship motions, shape, heat inflow from external sources, gas consumption of the engines, bunkering and schedule of the voyage). But as a general rule of thumb, a tank heel of 5% can be assumed for initial design considerations. However, the description of heel in the existing LNG bunkering guideline is adapted from the LNG Carrier loading process. Meanwhile, heel is only used as a propellant for the LNG-fueled ship. Consequently, in the case in the present study, it is assumed that the tank heel for the LNG receiving ship is 20% according to the conventional fuel bunkering operation. Tank pressure during bunkering could be maintained at an acceptable range by consuming LNG or by using the BOG control methods.

4) STS Bunkering Case

The size and capacity of bunker ships strongly depend on travel distances, requirements for multi-cargo capability, expected trade volumes, and characteristics of the receiving terminals. Generally, the capacity of the LNG bunkering ships ranges from 1,000 to 10,000 m³. As shown in Table 3.1, the IMO Type C pressure tank is installed on both of the ships, LNG tank volume of the bunkering ship is 4538 m³, diameter is 12.0 m, and the length is 40.12 m based on expert consultations. Hence, for the receiving ship with an LNG tank volume of 700 m³, the diameter is 8.0 m and the length is 13.93 m.

Table 3.1 Geometry for the LNG tanks of bunkering and receiving ships.

Parameter		Value	Tank Type
Bunkering Ship	Tank volume [m ³]	4538	IMO Type C/ Horizontal Cylinder
	Diameter [m]	12.0	
	Length [m]	40.12	
	Thickness of metal [m]	0.01	
	Thickness of insulation [m]	0.2	
	HTC of metal [W/m-K]	45	
	HTC of insulation [W/m-K]	0.0215	
	Ambient temperature [°C]	25	

Receiving Ship	Tank volume [m ³]	700
	Diameter [m]	8.0
	Length [m]	13.93
	Thickness of metal [m]	0.01
	Thickness of insulation [m]	0.15
	HTC of metal [W/m-K]	45
	HTC of insulation [W/m-K]	0.0215
	Ambient temperature [°C]	25

5) TTS Bunkering Case

For small ships, using tank truck to supply LNG to ships may be a feasible option. It is a mobile device that must be connected via the flexible hose to the receiving ship moored at the dockside when it arrives at the pre-determined location. This is a mobile device that must be connected via a hose to a receiving vessel parked at the dockside when it arrives at the intended location. The LNG truck's capacity varies from 40 to 80 m³, that depending on the tank design and regulations (DMA, 2012). The maximum allowable capacity allowed varies depending on national transportation and vehicle regulations and road infrastructure in each country. Therefore, for the present TTS bunkering case study, the tanks' capacity both the LNG tank truck and the receiving ship are set at 70 m³, the diameter are 3.0 m and the lengths are 9.90 m, as shown in Table 3.2.

Table 3.2 Geometry for the LNG tanks of tank truck and receiving ship.

Parameter		Value	Tank Type
LNG Tank Truck	Tank volume [m ³]	70	IMO Type C/ Horizontal Cylinder
	Diameter [m]	3.0	
	Length [m]	9.90	
	Thickness of metal [m]	0.01	
	Thickness of insulation [m]	0.1	
	HTC of metal [W/m-K]	45	
	HTC of insulation [W/m-K]	0.0215	
	Ambient temperature [°C]	25	
Receiving Ship	Tank volume [m ³]	70	IMO Type C/ Horizontal Cylinder
	Diameter [m]	3.0	
	Length [m]	9.90	
	Thickness of metal [m]	0.01	
	Thickness of insulation [m]	0.1	
	HTC of metal [W/m-K]	45	
	HTC of insulation [W/m-K]	0.0215	
	Ambient temperature [°C]	25	

3.2.2 Pipeline System Setup

Due to the increase of temperature and the drop of pressure, LNG evaporates into BOG in the pipelines, which is a multiphase flow problem. In this study, the Beggs-Brill equation of the homogeneous flow model was adopted to solve the multiphase flow problem in horizontal, vertical and inclined pipelines (Dale and James, 1973; Wu et al., 2019; Silva, 2016).

$$\frac{dp}{dz} = \frac{\frac{f\rho_n v_m^2}{2d} + \rho_s g \sin\theta}{1 - E_K} \quad (3.16)$$

where:

f = Two-phase friction

ρ_n = Mixture density (input liquid)

v_m = Mixture velocity

d = Diameter of the pipeline

ρ_s = Mixture density (corrected hold-up)

θ = Pipeline inclination from horizontal

E_K = Acceleration term

$$E_K = \frac{\rho_s v_m v_{sv}}{p} \quad (3.17)$$

where:

p = Pressure

v_m = Mixture velocity

v_{sv} = Superficial velocity of vapor phase

1) STS Bunkering Case

The bunkering pipeline system consists of LNG transfer pipes (bunker pipes) and vapor return pipes (BOG pipes) between the cargo tank of the bunkering ship and fuel tank of the receiving ship. The bunker pipes and BOG pipes are sized related to the design flow rates of the system. The design flow rate is related to the capacity, temperature and the pressure of LNG fuel tank, also other factors including the flow velocity limits, the BOG return capacity and bunkering time limit (ABS, 2014). Additionally, the flowrate depends on the achievable bunkering rate from the bunkering ship. In the study the maximum LNG transfer mass flow rate is set as 280,000 kg/h, and the LNG velocity is assumed to 6 m/s, as the mass density of LNG bunker is assumed to be 450 kg/m³ (Li, 2012). The diameter of the LNG bunker pipe is calculated as approximately 192 mm. Therefore, the diameter of the bunkering pipeline is set to 8 inch (200 mm) while that of the BOG pipeline is set to 4 inch (100 mm) to satisfy the pressure and BOG generation in the fuel tank of the receiving ship.

Mass flowrate:

$$\dot{m} = Q \times \rho = 280,000 \text{ kg/h} \quad (3.18)$$

Transfer rate:

$$Q = \frac{\dot{m}}{\rho} = \frac{280,000}{450} = 622 \text{ m}^3/\text{h at } V = 6 \text{ m/s} \quad (3.19)$$

Pipeline diameter:

$$D = \sqrt{\frac{4Q}{\pi V}} = \sqrt{\frac{4 \times 622}{\pi \times 6 \times 3600}} = 0.1916m \cong 192mm \quad (3.20)$$

where:

\dot{m} = LNG mass flow rate

Q = Volume flow rate

ρ = Mass density of LNG bunker

V = Velocity of LNG

D = Diameter of the pipeline

2) TTS Bunkering Case

In most current TTS bunkering operations, there are only the LNG transfer pipelines and no BOG return pipelines. When the receiving ship's pressure is higher than working pressure, since the LNG receiving ship is in a berthed state, the fuel gas consumption is low and the ship does not have a proper BOG treatment equipment, so the excess BOG have to be vented to the atmosphere. This not only causes waste of resources, but is also unfriendly to the environment. Therefore, in the pipeline system of the TTS bunkering case in this study, the same as the STS bunkering case, it is composed of two parts: LNG transfer pipes (bunker pipes) and vapor return pipes (BOG pipes). This technology has been successfully applied to liquefied natural gas (LNG) delivery for vehicles (PGS, 2013), and it is believed to be the trend of future TTS bunkering methods.

According to the LNG bunkering guidance of the European Maritime Safety Administrations (EMSA), in the 50 m³ TTS bunkering scenario, the flowrate of LNG is controlled at about 60 m³ per hour, and the diameter of the bunker hose used is two lines of 2 inch or one line of 3 inch. Due to the Equations 3.21-3.23, the diameter of the LNG pipeline was calculated as 69 mm. Hence, a 3-inch (75mm) LNG bunker hose is selected while that of the BOG pipeline is 2 inch (50 mm) to satisfy the pressure and BOG generation in the fuel tank of the receiving ship for the present standard TTS case study.

Mass flowrate::

$$\dot{m} = Q \times \rho = 30,000 \text{ kg/h} \quad (3.21)$$

Transfer rate:

$$Q = \frac{\dot{m}}{\rho} = \frac{30,000}{450} = 66.7 \text{ m}^3/\text{h at } V = 5 \text{ m/s} \quad (3.22)$$

Pipeline diameter:

$$D = \sqrt{\frac{4Q}{\pi V}} = \sqrt{\frac{4 \times 66.7}{\pi \times 5 \times 3600}} = 0.0687 \text{ m} \cong 69 \text{ mm} \quad (3.23)$$

3.2.3 Pump System Setup

In the LNG bunkering process, since the flow rate of the LNG pump is relatively stable, it can be considered as a steady facility, and its dynamic model is the same as the steady state model. In the dynamic simulation of the pump, the characteristic curve is needed. These characteristic curves are provided by the software company, Aspen Tech, and the characteristic curves did not change before and after the simulation.

In the present LNG bunkering scenario, the LNG pump is a cryogenic submersible pump. The model of the pump is as follows:

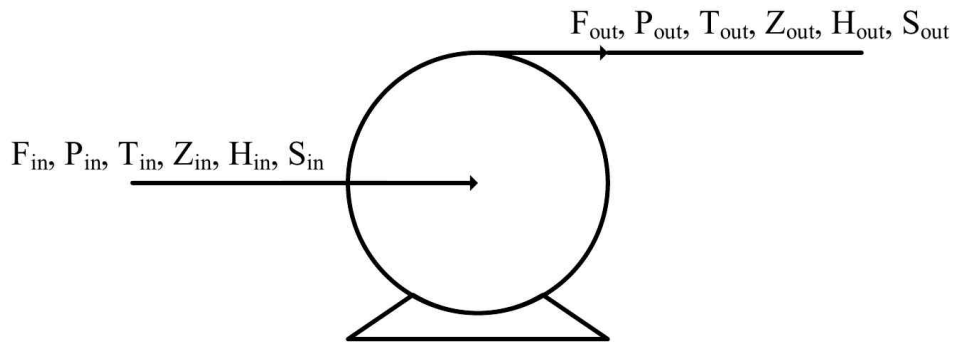


Fig. 3.2 Schematic diagram of LNG pump model.

Mathematical equations:

$$F_i = F_o \quad (3.24)$$

$$Z_i = Z_o \quad (3.25)$$

$$W = H_o - H_i = \frac{P_o - P_i}{\rho \cdot \eta} F_i \quad (3.26)$$

where:

F = LNG flow rate of the stream

Z = Molecular component of the stream

W = Power required (actual)

H = Enthalpy of the stream

P = Pressure of the stream

η = Efficiency of the LNG pump

Determination of LNG Flow Rate (STS & TTS Case)

The longer LNG is bunkered prior to use, and an increase in the number of times that it is transferred from one storage vessel to another increases the BOG generation. Several typical cases are used to determine the BOG generation change in different LNG bunkering time limits. The STS bunkering time limit sets of the cases correspond to 60, 90, 120 and 150 min., respectively. In the procedure of STS bunkering, the LNG mass flow rate adjusts to 72,000 kg/h when the level of the LNG tank of the receiving ship reaches 85%. Additionally, the initial LNG mass flow rate is calculated as 280,000, 180,000, 125,000 and 100,000 kg/h for each case. For the TTS bunkering case study, the bunkering time limit set to 50 min. according to the EMSA's guidance (EMSA, 2018). In the procedure of TTS bunkering, the control valve gradually adjusts the LNG mass flow rate to 0 kg/h when the level of the LNG tank of the receiving ship reaches 85%. In addition, the initial LNG mass flow rate is calculated as 30,000 kg/h. As mentioned

before, all the LNG bunkering procedure finished when the receiving tank reaches 90%. The mass flow rate for each case is shown in Table 3.3.

Table 3.3 LNG mass flow rates during different bunkering time limits.

Bunkering Method	Bunkering Time Limit [min.]	Initial Mass Flow Rate [kg/h]	Mass Flow Rate [kg/h] (after tank's level of receiving ship over 85%)
STS LNG Bunkering	60 <i>Standard Case</i>	280,000	72,000
	90	180,000	
	120	125,000	
	150	100,000	
TTS LNG Bunkering	50	30,000	30,000

3.3 Bunkering Process

1) STS Bunkering Case

The bunkering procedure by STS method was divided into two parts, namely startup and shutdown of the system as shown in Tables 3.4 and 3.5.

With respect to startup of the system modeling, it is necessary for several conditions to fit in the initial bunkering startup wherein the pressure and quality should be in a stabilized state and also a closed LNG bunker line should be present. During the procedure, five steps are involved in the modeling startup.

Table 3.4 Modeling of system startup.

Conditions for initial bunkering start-up	1) Conditions (pressure/quality) in the receiver tank and bunker tank should be in a stable state.
	2) BOG return line/LNG bunker line should be closed.
Process Change	1) Open BOG valve (bunker tank side and receiver tank side) for 10 s.
	2) Start the heat ingress in the bunker and receiver tank.
	3) Open LNG bunkering valve (receiver tank side) for 10 s.
	4) Start LNG bunkering pump (8.9 s after startup), and operate flow controller 9 s after the starting point.
	5) Open LNG bunkering valve (bunker tank side) for 10 s.

In the shutdown system, mass flow rate ramped down to 72,000 kg/h when the level of fuel tank for the receiving ship reached to 85%, and subsequently controller and pump should be cut-off when the conditions are satisfied. It should be noted that the simulation control is also under the aforementioned procedure during the cut-off.

Table 3.5 Modeling of system shutdown.

Process Change	1) When the level of LNG fuel tank for the receiving ship reaches 85%, the mass flow rate ramps down to 72,000 kg/h.
	2) When the level of the LNG fuel tank for the receiving ship reaches 89.99%, controller cut-off occurs.
	3) When the level of LNG fuel tank for receiving ship tank reaches 90%, the pump power cut-off occurs and all valves are closed for 20 s to prevent the surge phenomena.
Simulation Control	1) The size of the time step (Adaptive time stepping) is adjusted to 100 ms-1,000 ms.
	2) Setting of simulation stop: Finish bunkering and close all valves, then stop the system after 30 s.

2) TTS Bunkering Case

The bunkering procedure by TTS method was almost similar to the STS method. The only difference was when the level of LNG fuel tank for receiving ship tank reaches 90%, the pump power cut-off, directly.

3.4 Equation of State Selection & System Description

3.4.1 Equation of State Selection

Aspen HYSYS was used for the dynamic simulation to calculate and analyze the change in the BOG generation of the LNG fuel tank of the receiving ship for different bunkering scenarios.

With respect to the process modeling and thermodynamic analysis, we applied the Peng-Robinson Equation of State that can predict the thermodynamic properties of various hydrocarbons including LNG in a relatively accurate manner as follows (Soave, 1972; Stryjek and Vera, 1986) :

$$P = \frac{RT}{V_m - b} - \frac{a \times \alpha}{V_m(V_m + b) + b(V_m - b)} \quad (3.27)$$

where:

R = Gas constant

V_m = Molar volume

Here, the parameters α , a , b , and ω are defined as follows.

$$a = 0.45724 \frac{R^2 T_c^2}{P_c} \quad (3.28)$$

$$b = 0.07780 \frac{RT_c}{P_c} \quad (3.29)$$

$$\alpha = [1 + \kappa(1 - \sqrt{T_r})]^2 \quad (3.30)$$

$$\kappa = 0.37464 + 1.54336w - 0.26992w^2 \quad (3.31)$$

$$T_r = \frac{T}{T_c} \quad (3.32)$$

where:

P = Pressure

P_c = Temperature at critical point.

R = Gas constant

T = Temperature

T_c = Critical temperature

T_r = Critical pressure

V_m = Mole volume

a, b = Equation of state parameters

α = Function for reduced temperature and the acentric factor

κ = Function for the acentric factor

ω = Acentric factor

3.4.2 System Description (STS & TTS Bunkering Case)

Fig. 3.3 shows the schematic process flow diagram (PFD) of the STS LNG bunkering scenario and the TTS LNG bunkering scenario. The LNG bunkering model used for dynamic simulation was composed of two LNG storage tanks for bunker ship (tank truck) and receiving ship, a submersible LNG pump, the LNG bunkering pipeline (include an LNG cryogenic flexible hose), the BOG pipeline (include a BOG return cryogenic flexible hose), the emergency shutdown (ESD) valves, and the emergency release couplings (ERC). This research, only considers bunkering scenario that the number of LNG hose was 1. The initial conditions for each bunkering scenario will be introduced in the next section.

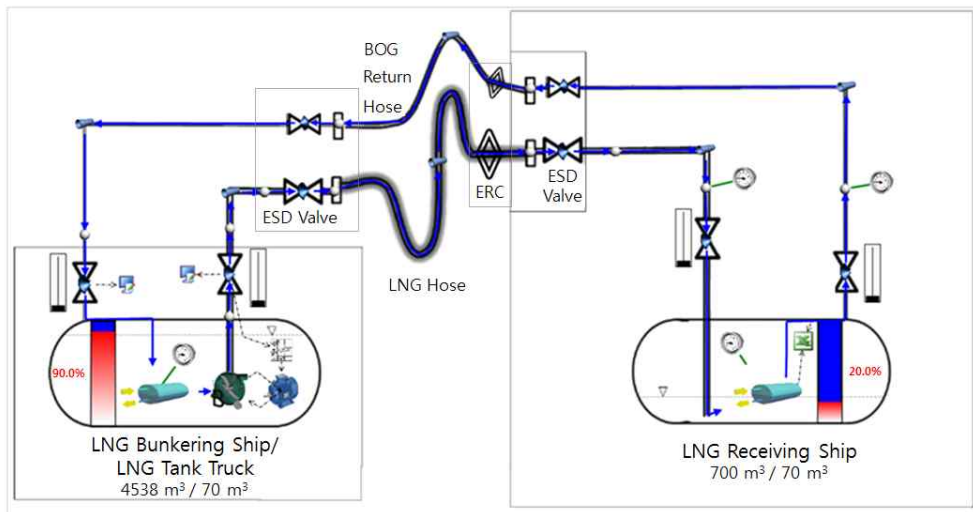


Fig. 3.3 Simplified process flow diagram of the STS/TTS LNG bunkering scenario (Begin Bunkering).

3.5 Initial Conditions

1) Standard Case (STS & TTS Bunkering Case)

Table 3.6 shows the initial conditions for the LNG tanks of bunkering ship (tank truck) and receiving ships. As recommended before, the LNG storage tank's capacities were 4,538m³ and 700 m³ for the bunkering and receiving ships, respectively. And for the TTS bunkering method, both the tank truck and the receiving ship's tank capacity are 70 m³. The case with an LNG bunkering time limit of 60 min. was selected as the standard simulation condition. For TTS bunkering method, the time limit was 50 min. The LNG tank level of the bunkering ship and receiving ship prior to commencing bunkering were filled to 90.0% and 20.0%, respectively. The initial temperature difference (ΔT) between the bunkering ship and receiving ship was 12.5 °C, with the pressure difference (ΔP) was approximately 3.0 bar.

Table 3.6 Initial conditions for the STS and TTS bunkering method (Standard).

		Bunkering ship (4,538 m ³)	Receiving ship (700 m ³)
STS LNG Bunkering (60 min.)	Tank level (%)	90.0	20.0
	Temperature (°C)	-147.0	-134.5
	Tank pressure (barg)	2.8	5.8
		Tank truck (70 m ³)	Receiving ship (70 m ³)
TTS LNG Bunkering (50 min.)	Tank level (%)	90.0	20.0
	Temperature (°C)	-146.8	-134.6
	Tank pressure (barg)	2.7	5.7

2) Case Study on Temperature Difference (STS Bunkering Case)

Table 3.7 shows the initial conditions for the LNG tanks of bunkering ship and receiving ships. From Case T1-T4, the initial temperature difference (ΔT) between the bunkering ship and receiving ship was 0.0 °C, 8.0 °C, 12.5 °C, 17.0 °C. The T3 ($\Delta T = 12.5$ °C) was set to the standard case.

Table 3.7 Initial conditions for the STS bunkering method (Temperature difference).

		Bunkering ship (4,538 m ³)	Receiving ship (700 m ³)
Case T1 ($\Delta T = 0.0$ °C)	Temperature (°C)	-147.0	-147.0
	Tank pressure (barg)	2.8	2.8
Case T2 ($\Delta T = 8.0$ °C)	Temperature (°C)	-147.0	-139.0
	Tank pressure (barg)	2.8	4.5
Case T3 ($\Delta T = 12.5$ °C) <i>Standard Case</i>	Temperature (°C)	-147.0	-134.5
	Tank pressure (barg)	2.8	5.8
Case T4 ($\Delta T = 17.0$ °C)	Temperature (°C)	-147.0	-130.0
	Tank pressure (barg)	2.8	7.3

3) Case Study on Methane Number (STS Bunkering Case)

The composition of the LNG supplied varies across different terminals, so that the MN also different. The LNG bunker in different MN would response to the LNG bunkering. Table 3.8 shows the initial conditions for the LNG tanks of bunkering ship and receiving ships by different methane number. From Case M1-M4, the initial MN in terminal USA – Alaska, Yemen, Qatar and Libya was 99, 82, 75 and 69. The M2 (MN = 82) was set to the standard case. The mass density is inversely proportional to the methane numbers.

Table 3.8 Initial conditions for the STS bunkering method (Methane Number) (Wärtsilä, 2018).

Case Number	LNG Terminal	Methane C1 (%)	Ethane C2 (%)	Propane C3 (%)	C4+ (%)	Nitrogen N2 (%)	Methane Number	Mass Density (kg/m ³)
Case M1	USA - Alaska	99.71	0.09	0.03	0.01	0.17	99	401.7
Case M2 <i>Standard Case</i>	Yemen	93.17	5.93	0.77	0.12	0.02	82	426.2
Case M3	Qatar	90.91	6.43	1.66	0.74	0.27	75	438.3
Case M4	Libya	82.57	12.62	3.56	0.65	0.59	69	466.4

3.6 Model Validation

As described in Section 2, the commercial software Aspen HYSYS is widely used for process dynamic simulation in the LNG industry, particularly in the field of BOG handling. It has been applied in many previous studies (Hasan et al., 2009; Lee et al., 2015; Effendy et al., 2019; Shariq et al., 2019; Park et al., 2016).

In this study, to verify the dynamic simulation model is conformed with the bunkering scenario, the amount of BOG generation was simulated, according to the initial temperature difference between bunker and receiving tank by applying HYSYS and Flownex. The temperature of the receiving tank was set at $-134.5\text{ }^{\circ}\text{C}$ as the standard initial temperature. Meanwhile, the temperature difference between bunker and receiving tank were 0.0, 8.0, 12.0 and $16.0\text{ }^{\circ}\text{C}$, respectively.

The Flownex is a commercial dynamic systems code used as the primary thermal-fluid simulation code by the Pebble Bed Modular Reactor Company (PBMR). The comparison with experimental data excellently with the average differences of all cases was less than 10% (Ravenswaay, 2006). Both of the simulations were performed under the same condition. As shown in Figure 3.7, the total mass of BOG generation was quite similar to those of the Flownex simulation.

The gap range for the results validated in each initial temperature difference was below 15%. Especially when the initial temperature difference (Δt) was $12.0\text{ }^{\circ}\text{C}$, the gap range was below 2%. Therefore, the HYSYS

dynamic simulation could be used to conduct the dynamic behaviors of the STS and TTS LNG bunkering procedure. The result of the model validation was shown in Fig. 3.4.

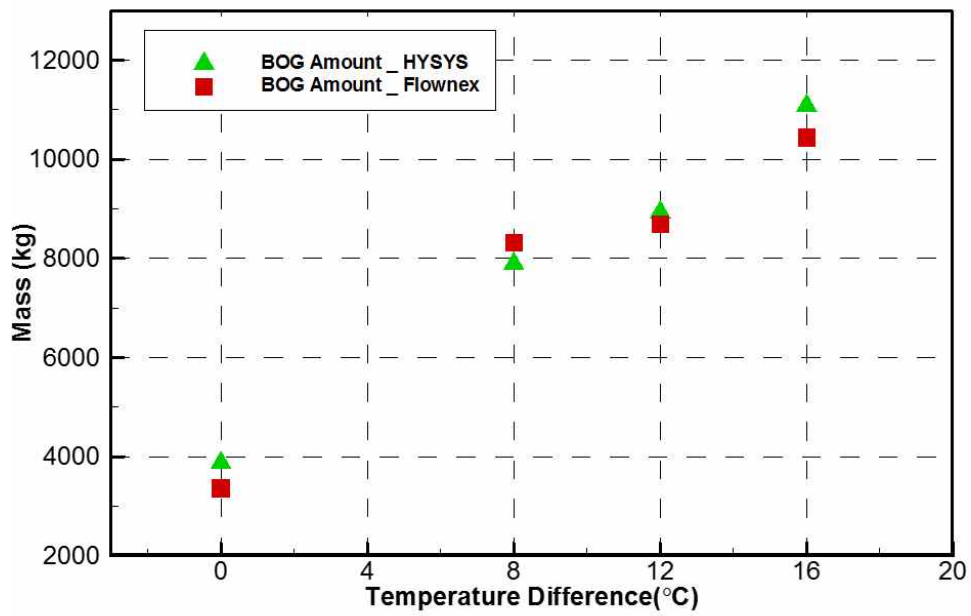


Fig. 3.4 Comparison of HYSYS and Flownex simulation predicted the amount of BOG generation.

Chapter 4 Results and Discussion

4.1 Disturbance of Temperature

To understand the parametric effects of temperature and pressure on the bunkering limit, it is helpful to consider an example where the LNG and vapor are not consumed from the tank. In this case, the LNG fuel tank was a closed system and remained at a saturated condition, which means that the liquid and vapor were in equilibrium. Even though the tank was insulated, some heat leaked into the tank and caused an increase in the liquid and vapor temperatures, while remaining in a saturated condition.

1) Transient BOG variation

The temperature difference between the two liquids can be significant; thus, the saturated vapor pressures will also be different. If the vapor spaces of the bunker's colder tanks and the receiver's warmer tanks are interconnected directly prior to the commencement of the LNG transfer, the receiving tank is likely to depressurize rapidly due to the condensation of vapor.

Similarly, if the LNG of the bunker vessel is cold, it will be pumped into a warm tank of the receiving vessel, and a considerable amount of flash gas might be generated as the cold LNG is warmed by the contents of the tank. Vapor control during bunkering is critical and can be handled in several different ways, depending on the supplying and receiving capabilities of the system and the LNG conditions in the tanks (ABS, 2014).

Fig. 4.1 shows the relationship between the variation of the BOG flowrate in the receiving tank, and the temperature difference between the two tanks. At the beginning of the bunkering procedure, when the pump starts, a great mass of heat ingress to the LNG transfers from the bunkering tank into the receiving tank. The amount of generated BOG is proportional to the temperature difference (Δt) between the bunkering and receiving tanks.

As shown in the figure, the amount of filling in the receiving tank increased, while the temperature difference decreased. Then, the generated BOG gradually decreased. At the end of the bunkering procedure, the BOG flow rate decreased rapidly when the pump stopped due to LNG no longer being transferred into the receiving tank.

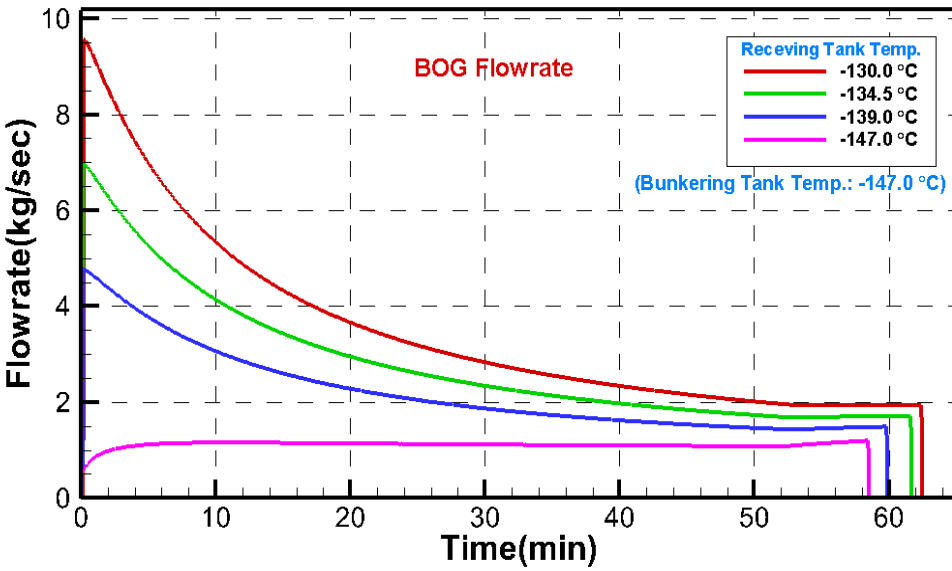


Fig. 4.1 BOG flow rate of receiving tank.

The LNG density decreased as the temperature increased. If the receiving tank was nearly full, the storage space available for BOG was relatively small. Therefore, the increase in liquid volume due to lower density could significantly reduce the available volume of vapor space. This decrease in available BOG volume as a result of temperature changes resulted in higher vapor pressure.

2) BOG return

Heating is counteracted by the cooling effect of evaporation as the LNG boils off. The gas boils off in order to fill the lost volume of the LNG or vapor in the tank, while maintaining the LNG liquid and vapor in equilibrium at the cooler saturated temperature and pressure. Therefore, slow or no removal of LNG and BOG from a tank can cause the tank temperature and the vapor pressure increase from the heat flux into the tank, while fast removal without forced generation of boil-off gas can cause the LNG tank temperature to decrease (ABS, 2014).

It is important to know the temperature in the LNG fuel tanks, in comparison to the bunkered temperature of the LNG, because the temperature difference can have a significant effect on the vapor control process.

In this study, the receiving LNG storage tank was stored and transported under the LNG conditions as a cryogenic liquid (-162 °C). The capacity of the receiving tank was 700 m³. The LNG evaporated at temperatures above its boiling point, while the boil-off-gas generated similar to any other liquid. BOG emerged from the heat ingress into the LNG during shipping, storage, and on/off loading operations (Dobrata et al., 2013).

In this simulation, BOG was caused by the temperature difference (Δt) between the bunkering and receiving tanks. As the quantity of the BOG increased, the pressure in the LNG receiving fuel tank also increased. At this point, it was required to control the BOG increase in order to retain the LNG storage tank pressure within the range of safety.

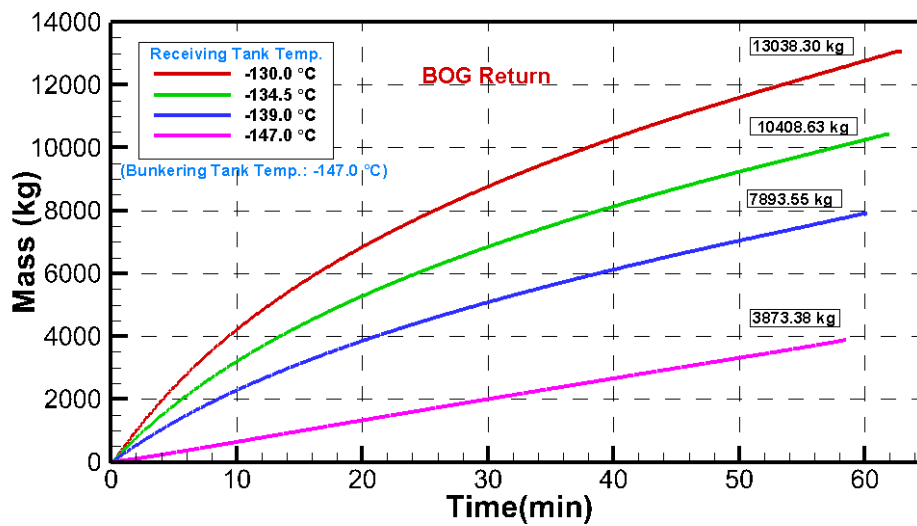


Fig. 4.2 Mass of BOG return from receiving tank.

Fig. 4.2 shows the relationship between the variation of the BOG return mass from the receiving tank for the temperature difference (Δt) between the bunkering and receiving tanks. It can be seen from the plot that the amount of BOG return mass from the receiving tank was proportional to the temperature difference (Δt) between the bunkering and receiving tanks. From the plot, the temperature difference (Δt) between the bunkering tank and the receiving tanks could be observed at 0.0 °C, 8.0 °C, 12.5 °C, and 17.0 °C, while the mass of the BOG that returned from the receiving tank was 3,873.38 kg, 7,893.55 kg, 10,408.63 kg and 13,038.30 kg, respectively.

3) Variations of supply and receiver tank pressure

For the safety system, if the tank temperature was allowed to increase unchecked, the pressure in the tank would increase to the point where the pressure relief valves opened. The temperature of the LNG at this point was the reference temperature. Here, the reference temperature was the temperature corresponding to the saturated vapor pressure of the LNG at the set pressure of the pressure relief valves (ABS, 2014). Since the density of the LNG at the reference temperature was lower than the density at the bunkering temperature, it was clear that the bunkering limit would always be lower than the filling limit.

Fig. 4.3 shows that at the initial bunkering, the pressure of the receiving tank increased due to the excessive BOG resulting from heat ingress. However, the rate of BOG generation decreased with the increase of LNG bunkering. When the filling rate of the receiving tank reached 85%, the pressure rate in the bunkering tank increased due to the decreasing LNG flow rate, which is shown in Fig. 4.4. If the LNG in both tanks had a similar temperature, and as the receiving ship's fuel tank was filled with LNG, the LNG displaced an equal volume of BOG that was already in the tank. Then, the vapor had to be condensed to liquid or transferred from the receiving fuel tanks in order to eliminate the excessive pressure buildup. Therefore, the vapor control in the two tanks could be accomplished by a BOG return line, which allowed the displaced vapor from the receiving tank to be returned to the bunkering vessel's tank. Moreover, the variation of transient pressure for both tanks was proportional to the temperature difference (Δt) between the bunkering and receiving tanks.

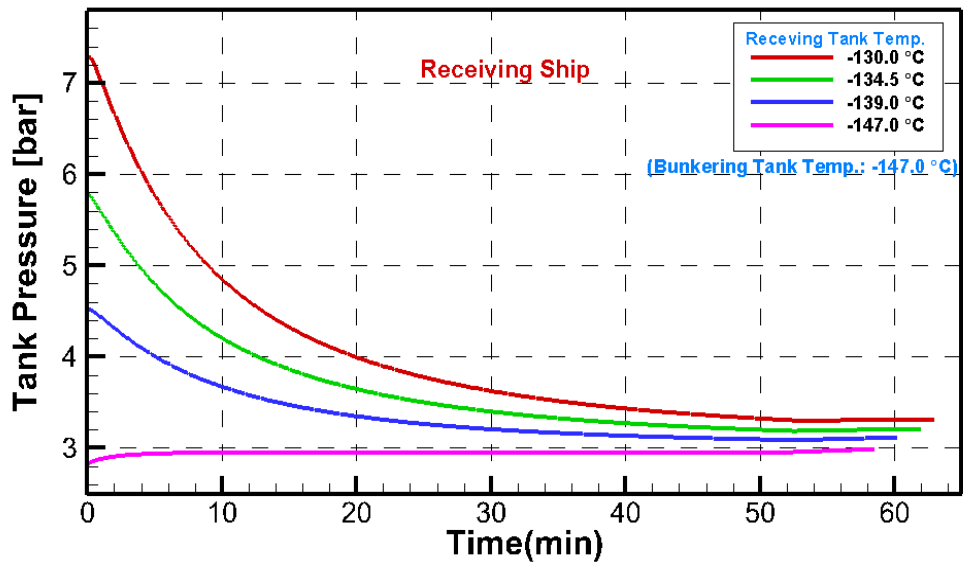


Fig. 4.3 Variations of receiving tank pressure.

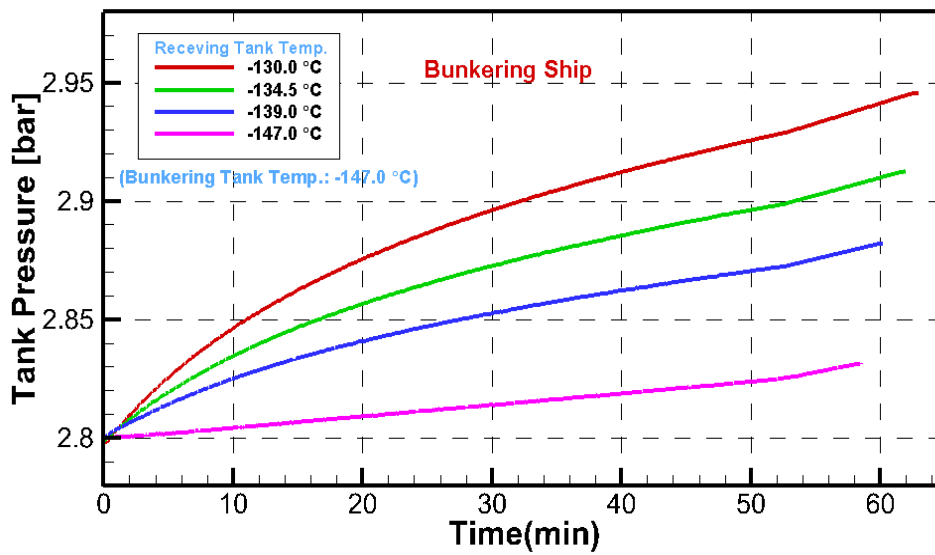


Fig. 4.4 Variations of bunkering tank pressure.

4) Total LNG bunkering amount

Some vessels may require a shorter bunker time than others, depending on their operating profile. Depending on the size of the fuel tanks and frequency of bunkering, the owners may wish to maximize the bunker rate.

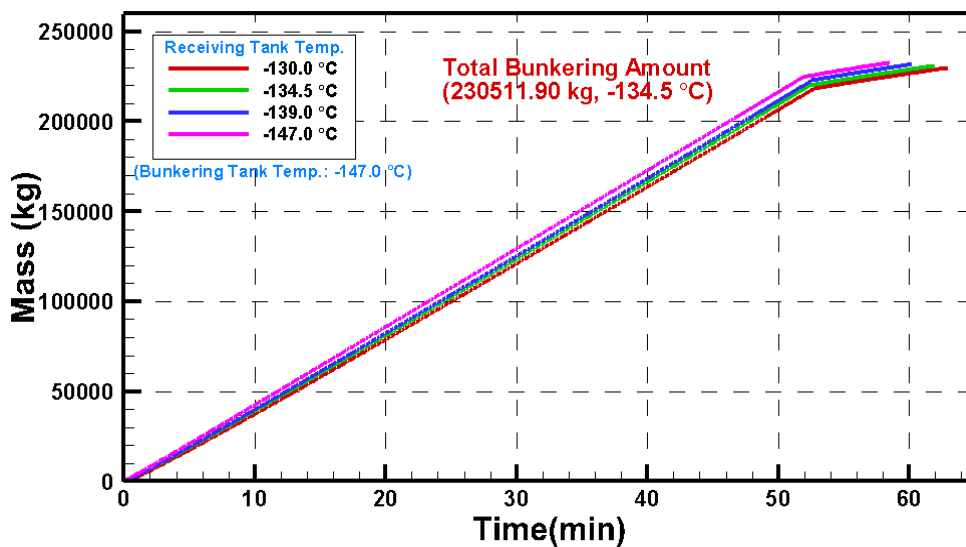


Fig. 4.5 Total LNG bunkering amount.

Fig. 4.5 presents the total amount of LNG bunkering with respect to bunkering time and temperature difference (Δt). For the typical case with a duration of 60 min., the total amount of LNG bunkering was 230,511.9 kg, when the filling rate of the receiving tank reached 90%. Then, the amount was inversely proportional to the temperature difference (Δt) between the bunkering tank and receiving tank due to the generation of BOG during the LNG bunkering scenario.

4.2 Disturbance of Methane Number

1) Transient BOG variation

Fig. 4.6 shows the variation of the BOG flowrate in the receiving tank with different MN. At the beginning of the bunkering process, when the pump was started, a large amount of heat entering the LNG was transferred from the bunkering ship to the receiving ship. In all cases, the amount of BOG generation was almost the same.

As shown in the figure, as the receiving ship filling up, the BOG flow rate decreases. Then, the BOG generation was gradually reduced. At the end of the bunkering process, as the LNG is no longer transported to the receiving ship, the BOG flow rate dropped rapidly as the pump shutdown. In addition, the total bunkering time was proportional to the MN due to the higher the MN, the more BOG generated.

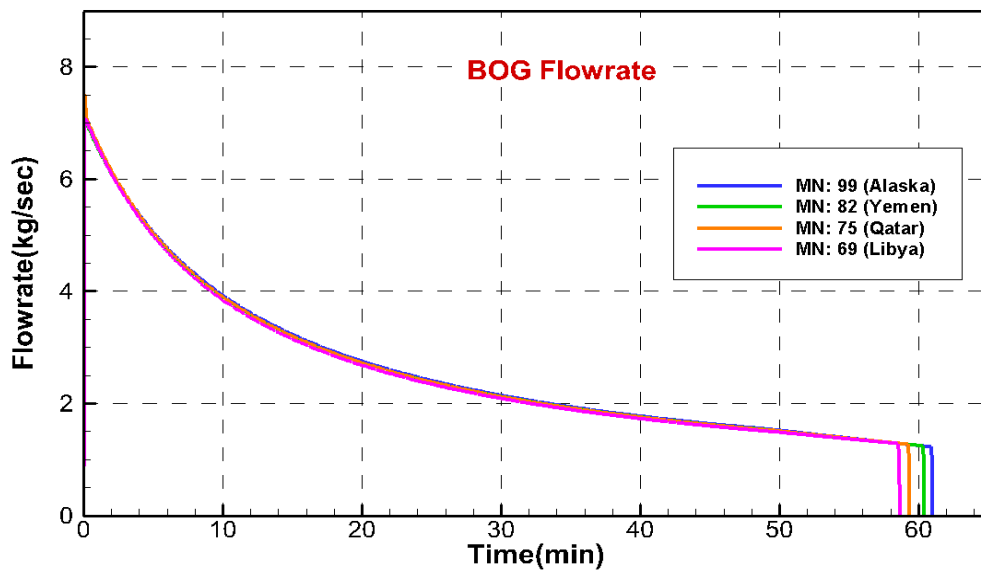


Fig. 4.6 BOG flow rate variation of receiving ship based on different methane number

2) BOG generation

During the LNG bunkering process, BOG is caused by the heat ingress to the tank and the temperature difference and between the bunker tank and the receiving tank. As the BOG increases, the pressure on the LNG receiving tank also increases. Therefore, in order to avoid the overpressure of the LNG storage tank, it is necessary to handle the BOG.

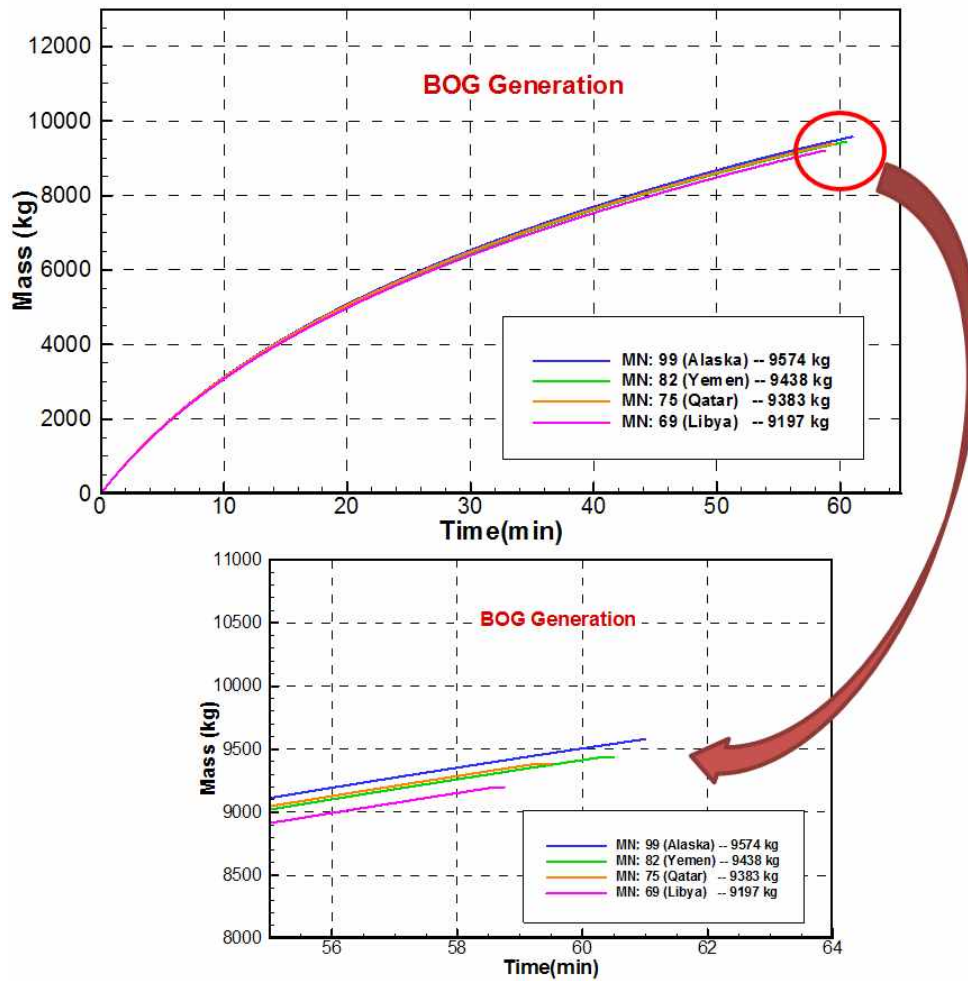


Fig. 4.7 Mass of BOG return from receiving tank.

Fig. 4.7 shows the variations of the BOG generation in the receiving tank with different MN. As can be seen from the figure, the amount of BOG generation from receiving ship is increasing rapidly and proportionally with the MN in each case. The case of Alaska generated the largest amount of BOG (9,574 kg). Meanwhile, the BOG generation for Yemen case was roughly consist with Qatar case due to the densities of LNG bunker were approximated. The amount of BOG generation for Yemen, Qatar and Libya was 9,438 kg, 9,383 kg and 9,197 kg, respectively.

3) Variations in the bunker and receiver tank pressure

Fig. 4.8 shows that at the initial bunkering, the pressure of receiving ship is under the condition of the increased pressure due to excessive BOG resulting from the heat ingress. However, the amount of BOG generation decreases due to the increasing of LNG bunkering. When the tank level of receiving ship reached at 85%, the pressure rate in bunkering ship is increased due to decreased of LNG flowrate, which could be seen in Fig. 4.9.

In in order to avoid the overpressure in the LNG storage tank of receiving ship, the BOG had to be condensed to liquid by the re-liquefaction equipment or transferred from the receiving ship. Consequently, in the present study, the BOG handling of the two storage tanks was done by passing through the BOG return pipe, which allowed the BOG transferred from the receiving ship to the cargo tank of the bunkering ship. In addition, the transient pressure changes of the two tanks are proportional to the MN of the LNG bunker in this simulation.

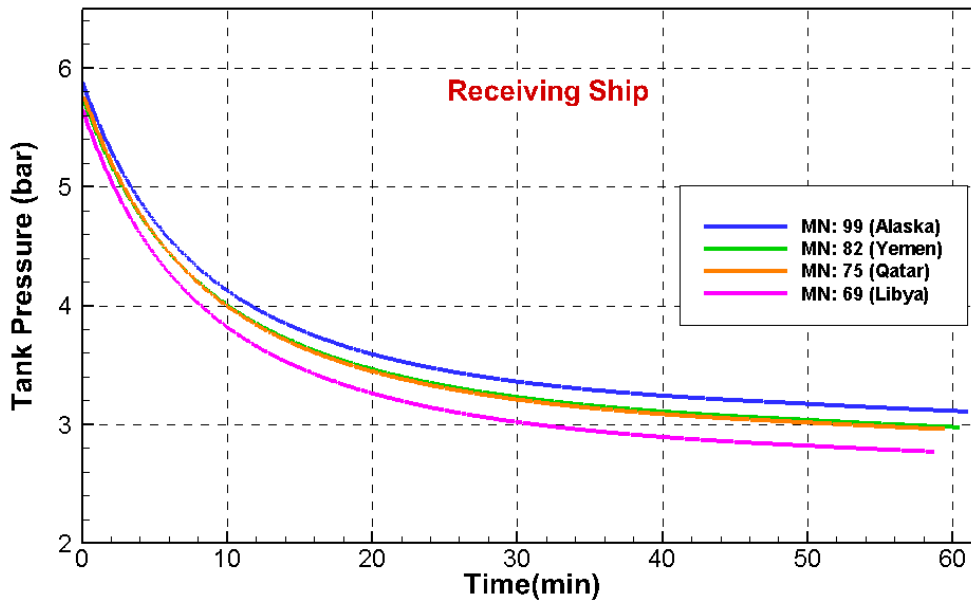


Fig. 4.8 Variations of receiving tank pressure.

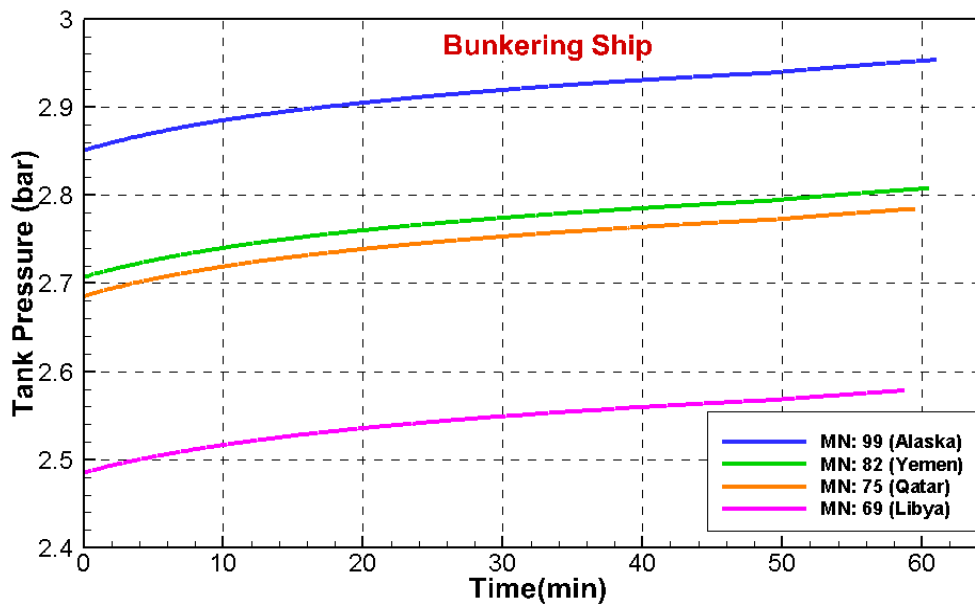


Fig. 4.9 Variations of bunkering tank pressure.

4) Total LNG bunkering amount

As shown in Fig. 4.10, the total bunkering amount means the total mass of LNG that transferred from the bunker ship to the receiving ship during the entire LNG bunkering process minus the total mass of BOG generation that passing through the BOG return pipeline. The total bunkering amount is significantly related to the LNG bunker in different MN due to the mass density difference in different MN. The gap between the maximum bunkering amount and the minimum bunkering amount was 14%. In the Libya case, the maximum bunkering amount corresponds to 258,663.3 kg. Furthermore, the trend of the total bunkering amount at different MN was reverse proportionally to the change in the BOG generation. This is because the bunker with the higher mass density, the more LNG will be transferred from the bunkering ship to the receiving ship.

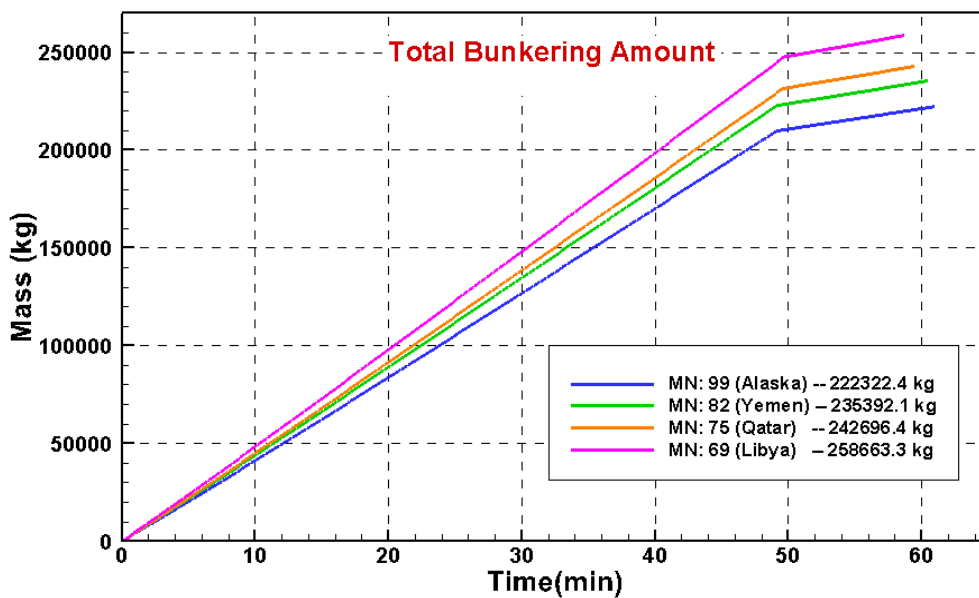


Fig. 4.10 Total LNG bunkering amount.

4.3 Optimal BOG Generation in Different Bunkering Time Limits

1) Transient BOG variation

The property differences between the bunkered LNG and the LNG in the receiving ship can cause the problems that require carefully control of the BOG. In the most cases, the bunkering operation consists of filling a colder LNG (LNG bunkering ship) into a tank that contains a relatively warmer LNG (LNG-fueled ship).

The LNG density decreased when the temperature increased. If the receiving LNG tank was nearly full, the storage space for BOG was relatively low. Therefore, the increase in liquid volume due to lower density can significantly reduce the available volume of vapor space. The decrease in available BOG volume due to temperature changes increased the vapor pressure.

Fig. 4.11 shows the BOG flow rate variation for different bunkering time limits. At the beginning of bunkering, a high amount of heat exchange was generated when LNG with low temperature was injected to the receiving ship, and thus the BOG flow rate peaked to 7 kg/s. In the initial 20 min. for all the bunkering cases, the BOG flow rate was directly proportional to the bunkering time limit, i.e., an increase in the bunkering time limit increased the BOG flow rate that was generated. Conversely, the BOG flow rate was inversely proportional to the bunkering time limit after 20 min. At the end of the bunkering scenario, the BOG flow rate corresponded to 1.24, 0.55, 0.322, and 0.267 kg/s for the time limits corresponding to 60, 90, 120 and 150 min., respectively.

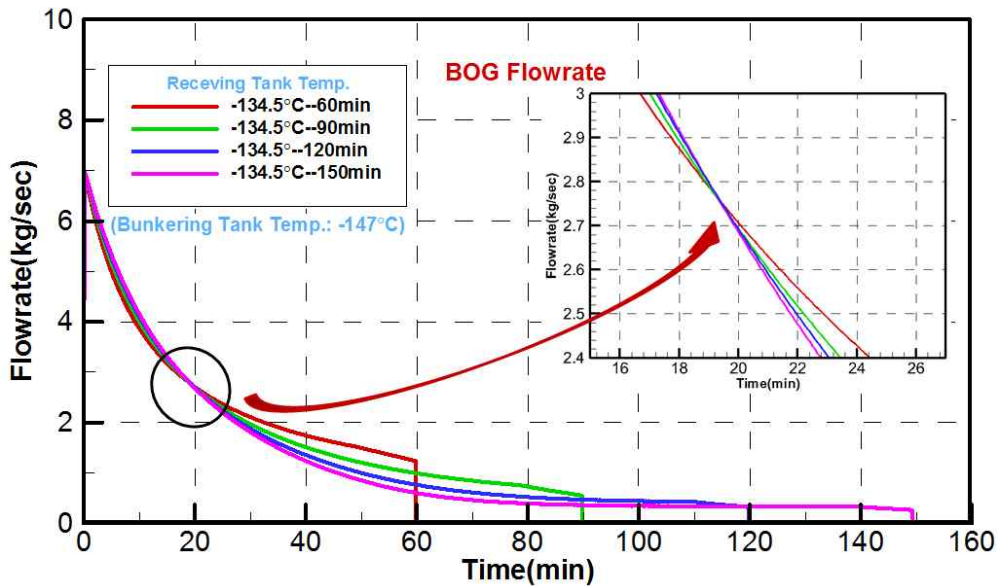


Fig. 4.11 BOG flow rate variation based on different bunkering time limits.

2) BOG generation

Heating is counteracted by the cooling effect of evaporation as the LNG boils off. The gas boiled to replace the reduction in the volume of the LNG or vapor in the tank while maintaining the LNG liquid and vapor in equilibrium at the cooler saturated temperature and pressure (ABS, 2014).

Therefore, no removal or slow removal of LNG and boil-off gas from the tank can increase the temperature and vapor pressure of the tank by the reason of heat flux into the tank, while rapid removal without forced generation of BOG could cause the LNG tank temperature to decrease. As a result, it is important to measure the temperature in the LNG fuel tanks when compared to the bunkered temperature of the LNG since temperature differences can significantly affect the vapor control procedure.

In the study, the receiving LNG was stored and transported under the LNG conditions as a cryogenic liquid. The capacity of the receiving ship was 700 m³. The LNG evaporated at temperatures above its boiling point while the boil-off-gas was generated in a manner similar to that for any other liquid. The BOG emerged from the heat ingress into the LNG during shipping, storage, and on/off loading operations (Dobrata et al., 2013).

Fig. 4.12 shows the changes in the BOG generation for four different bunkering time limits. In the initial 35 min., given the build-up of BOG flow rate, the BOG generation was proportional to the bunkering time limit. In order to optimally determine the relationship between the time limit and the BOG generation, the bunkering time limit was set as simulated for every alternate 10 min. in a period ranging from 50 min. to 150 min. based on the BOG generation to determine the optimal bunkering time limit.

As shown in Fig. 4.13, in the period from 50 min. to 120 min., the amount of BOG generation change increased with increases in the bunkering time limit and peaked to 10535.24 kg at 120 min. and subsequently reduced gradually.

Additionally, a decrease in the time limit decreases the amount of BOG generation. However, the bunkering time limit did not shorten without a limit given the restrictions such as the pump capacities and pipeline diameters. Thus, this suggests that the bunkering time should be controlled within 120 min. to avoid additional BOG generation when the capacity of the pump exceeds 100,000 kg/h. Conversely, the bunkering efficiency could be efficiently improved to reach the optimal time limit when the pump's capacity is lower than 100,000 kg/h.

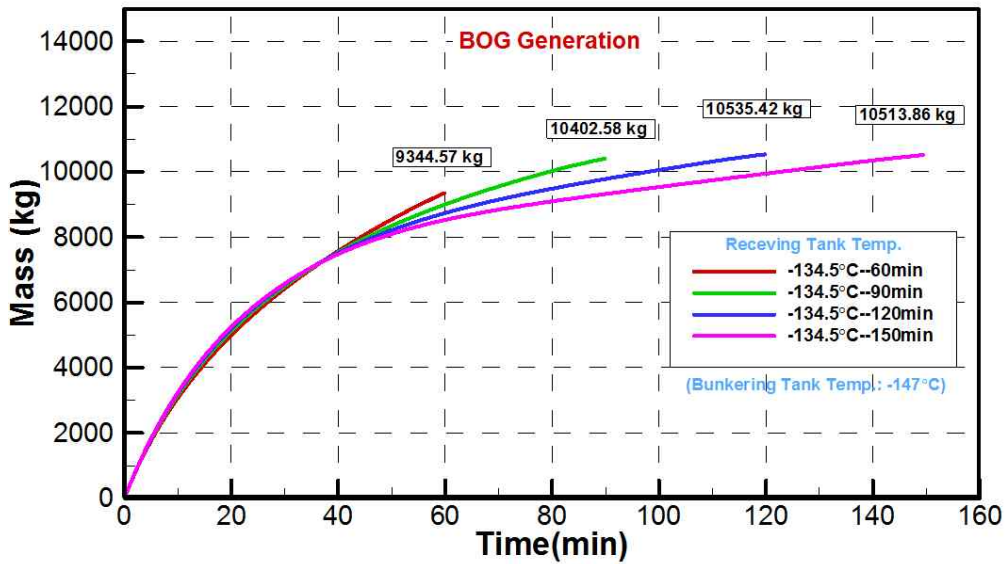


Fig. 4.12 Effect of bunkering time on BOG generation at the receiving LNG storage tank.

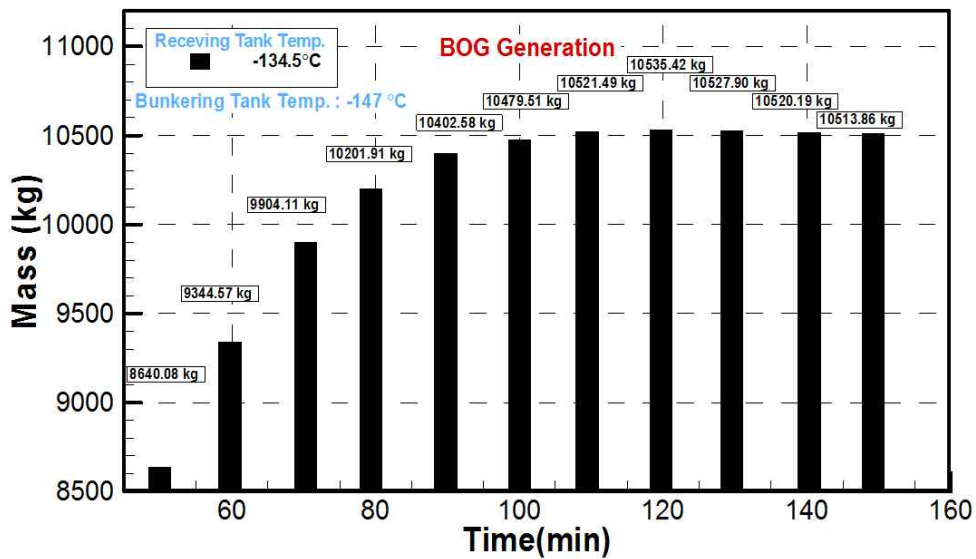


Fig. 4.13 BOG profile during bunkering operation for the BOG from the receiving tank at different bunkering time limits (50–150 min.).

3) Variations in the bunker and receiver tank pressure

With respect to the safety system, if the tank temperature was allowed to increase in an unchecked manner, the pressure in the tank increased to the point where the pressure relief valves open. The temperature of the LNG at this point corresponded to the reference temperature. The reference temperature was the temperature corresponding to the saturated vapor pressure of the LNG at the set pressure of the pressure relief valves (ABS, 2014). Evidently, the bunkering limit was always lower than the filling limit since the density of the LNG at the reference temperature was lower than the density at the bunkering temperature.

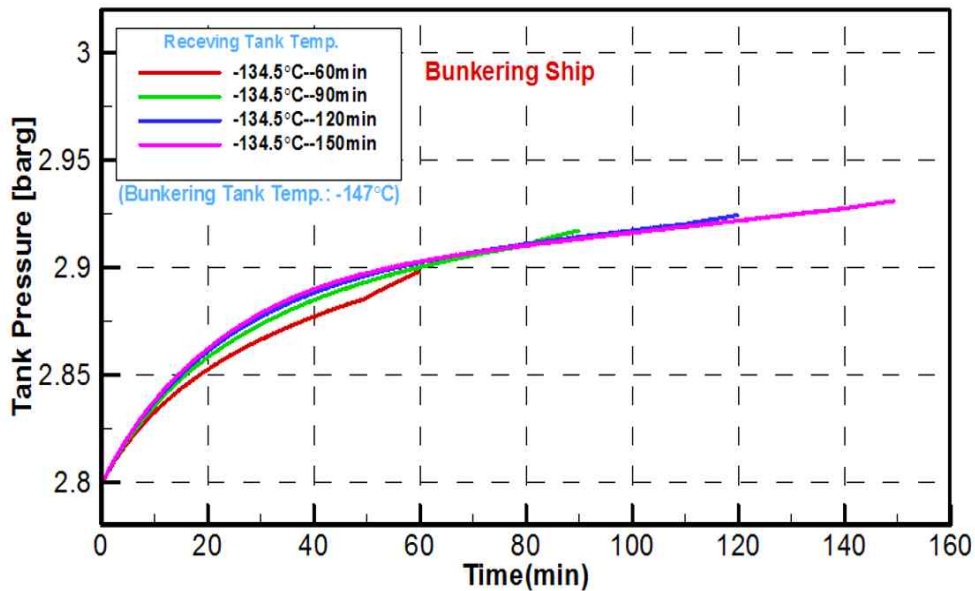


Fig. 4.14 Pressure variation in the bunker cargo tank of the bunkering ship during the bunkering operation at different bunkering time limits.

As shown in Fig. 4.14, the variations in the bunker tank pressure are not obvious when compared with the receiving ship. This is due to the following reasons: On one side, given the tank pressure difference, the vapor was only unilaterally transferred into the bunker tank from the fuel tank of the receiving ship during the bunkering procedure.

On the other side, the BOG generated from the bunker tank itself was limited, and the bunker tank was capacious. The variation in the tank pressure for the bunkering ship increased from 2.8 barg initially to 2.90–2.93 barg at the end of each case, and the ending pressure was directly proportional to the bunkering time limit. Specifically, with respect to the level of the fuel tank for the receiving ship prior to 85%, the tank pressure increased relatively quickly, and the variation was proportional to the bunkering time limit. This is because the mass and pressure of the outflowing LNG increased slowly while an increase in the bunkering time limit decreased the discharging LNG rate. Additionally, when the receiver tank reached 85%, the pressure in the bunker tank increased due to decreases in LNG flow rate.

As shown in Fig. 4.15, the fuel tank pressure of the receiving ship is directly proportional to the time limit in the first 20 min. in each case. The reasons are as follows: first, the LNG in bunker tank was transferred to the fuel tank of receiving ship with decreases in the temperature and pressure. Second, the aforementioned pressure in the fuel tank decreased quickly since the BOG pipelines were well connected with the bunker tank. Finally, the pressure decreased if the fuel tank could obtain a higher LNG transfer flow rate during the bunkering procedure.

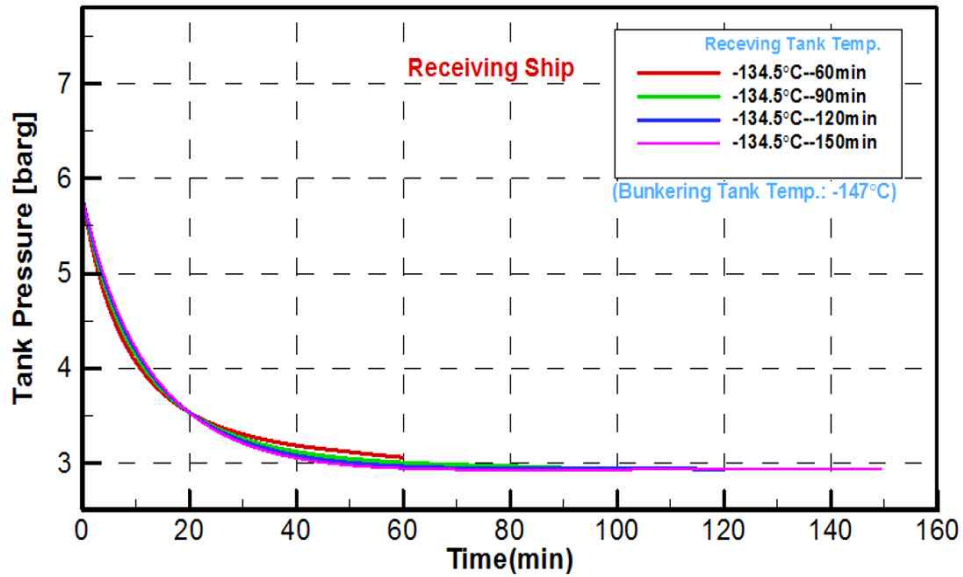


Fig. 4.15 Pressure variation in the fuel tank of the receiving ship during the bunkering operation at different bunkering time limits.

Conversely, the tank pressure of the receiving ship was inversely proportional to the time limit after 20 min. It was observed that the pressure variation in fuel tank for the receiving ship changed significantly, and the pressure reduced from 5.77 barg at the beginning to the 2.94-3.06 barg in the end of each case. The tank pressure difference between bunkering and receiving ship decreased with increases in the bunkering time limit.

4) LNG flow rate and total LNG bunkering amount

A few ships may require a shorter bunkering time when compared to others based on their operating profile. Based on the frequency of bunkering and the size of the fuel tanks, the owners may wish to maximize the bunkering rate (Shao et al., 2018).

As shown in Fig. 4.16, the LNG flow rates in each case are different before the level of fuel tank reaches 85% in different bunkering cases (Take Table 2 as reference) while the flow rate reduces uniformly to 72,000 kg/h when the level of fuel tank exceeds 85%. When the level of fuel tank reached 90%, the pump stopped working, the valve closed, and the entire bunkering procedure was completed.

As shown in Fig. 4.17, the total bunkering amount refers to the total mass of LNG that transferred from the bunkering ship to the receiving ship during the entire LNG bunkering procedure minus the total mass of BOG generation that passing through the BOG return pipeline. The total bunkering amount is not significantly related to the bunkering time limit. The gap between the maximum bunkering amount and the minimum bunkering amount was less than 0.5%. In the case of 120 minutes, the maximum bunkering amount corresponds to 231.8 tons.

Meanwhile, the trend of the total bunkering amount at different bunkering time limits was consistent with the change in the total amount of BOG. This is because the bunkering time limit with the higher BOG amount, the more LNG will be transferred from the bunkering ship, correspondingly.

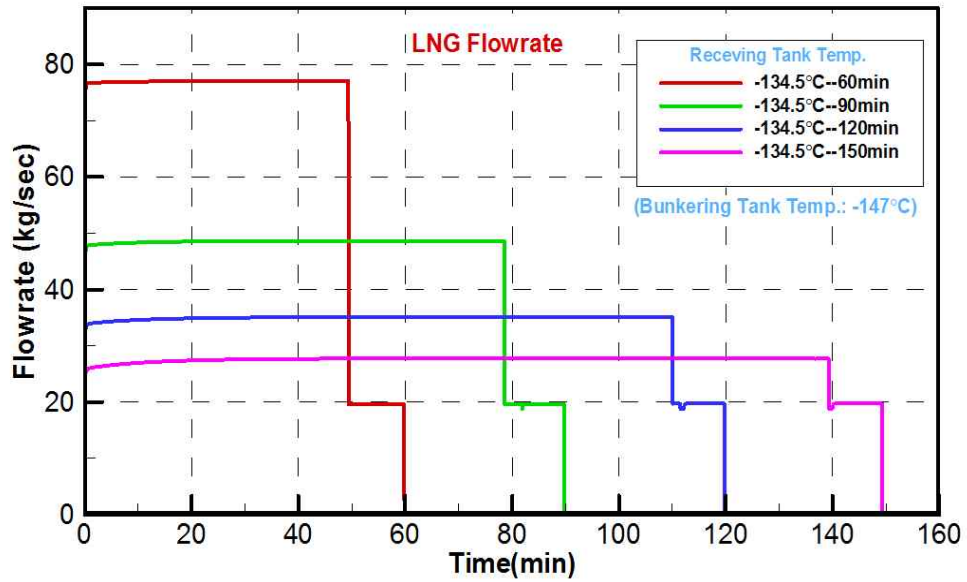


Fig. 4.16 Relation between the LNG flow rate and the respective bunkering times.

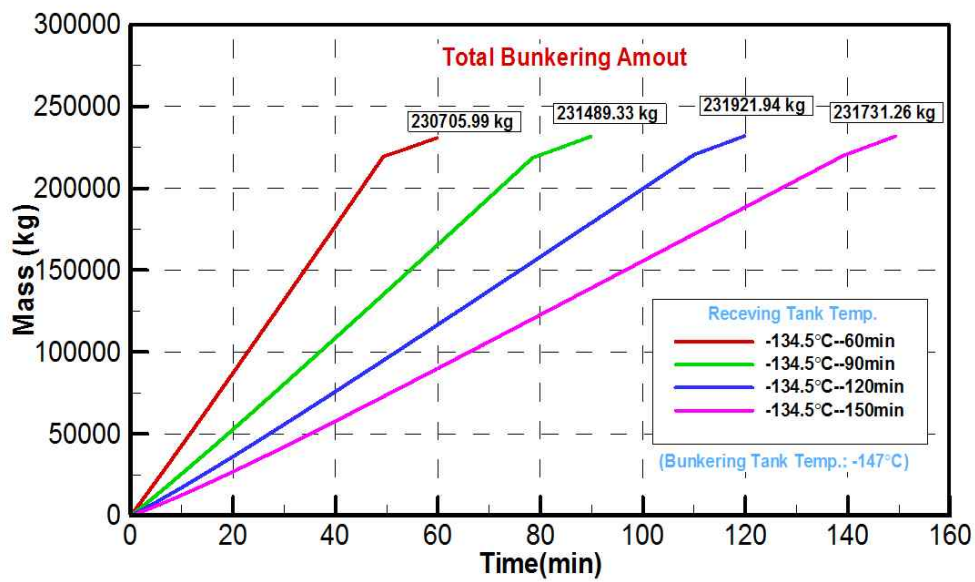


Fig. 4.17 Total bunkering amounts with respect to different bunkering times and pump stops.

5) Summary

As shown in Table 4.1, BOG is considered as a core consideration throughout the STS LNG bunkering procedure. The total amount of BOG generation by different bunkering time limits is not the same. Among them, the total amount of BOG is the highest in the 120 min. case, whereas in the 60 min. case is the least. When the bunkering time limit is less than 120 minutes, the BOG amount is proportional to the bunkering time limit. Therefore, the shorter the bunkering time limit is, the more benefits will generate in safety, efficiencies and others. Since the heat transfer can be carried out through the BOG return pipeline, the longer the time limit, the smaller the temperature difference between the two ships. Hence, with the increase of the bunkering time limit, the pressure difference between the bunkering ship and the receiving ship decreases. For the total bunkering amount, it is consistent with the trend of the total BOG amount.

Table 4.1 Quantity of state respect to different bunkering time limits (Finish Bunkering).

Bunkering Time Limit (Min.)		60	90	120	150
BOG Amount (kg)		9344.57	10402.58	10535.42	10513.86
Tank Pressure (Barg)	Bunkering Ship	2.90	2.93	2.93	2.93
	Receiving Ship	3.06	2.99	2.97	2.94
Total Bunkering Amount (kg)		230705.99	231489.33	231921.94	231731.26

6) Calculation for mass of BOG amount

As mentioned in before, a dynamic simulation was carried out for the amount of BOG generated in the 50-150 min. STS LNG bunkering process. However, through the dynamic simulation method, it is unrealistic to calculate the BOG amount generated in any bunkering time limit. Therefore, based on the simulated data, the Sigmoidal Weibull function type 2 (SWeibull 2) in OriginPro 2017 software (OriginLab Cor., Northampton, MA, USA) was used to fit the simulated data (Seo et al., 2017; Nguyen et al., 2017), as shown in Fig. 4.18.

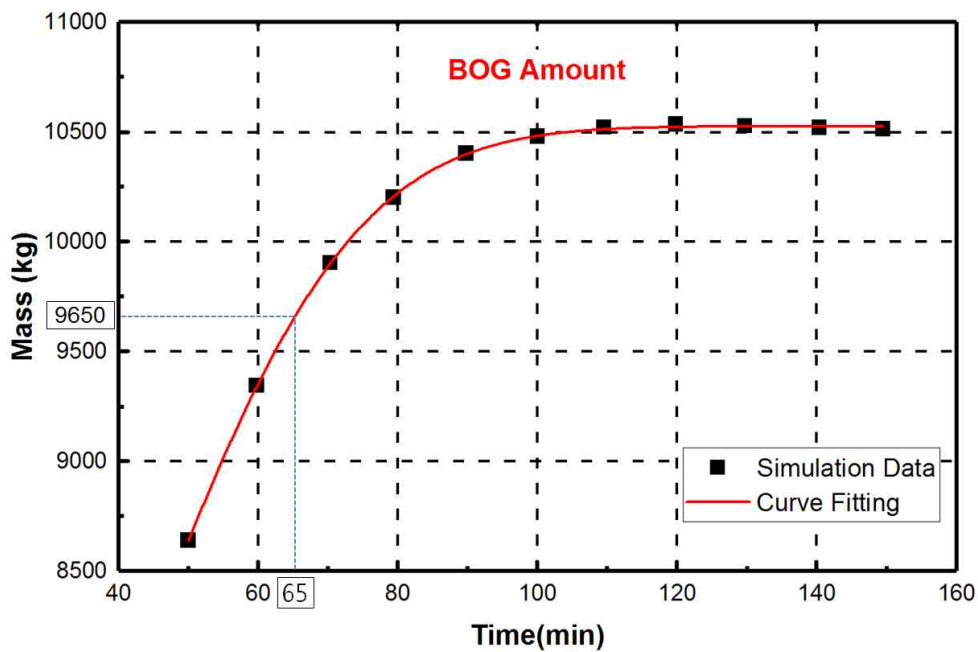


Fig. 4.18 Mass of BOG generation amount and its curve fitting result.

According to the fitting curve, the mass of BOG generation amount could be performed simply by the following equation:

$$\dot{m}_{BOG} = A - (A - B)e^{-(kt)^d} \quad (4.1)$$

As shown in Fig. 4.18, the fitting curve is quite consistent with the results of dynamic simulation. It has the advantage of suitable for development region. A correlation of the simulated data using the above formulation, and with the least squares estimates parameters A , B , d and k of 10,526.69, 6,087.63, 2.4313 and 0.0188, respectively. The \dot{m}_{BOG} presents the mass of BOG generation amount within the STS LNG bunkering time. For example, the value of BOG amount when the bunkering time at 65 min. is approximately 9,650 kg.

4.4 Optimal BOG Generation in Different Pipe Diameter Ratio

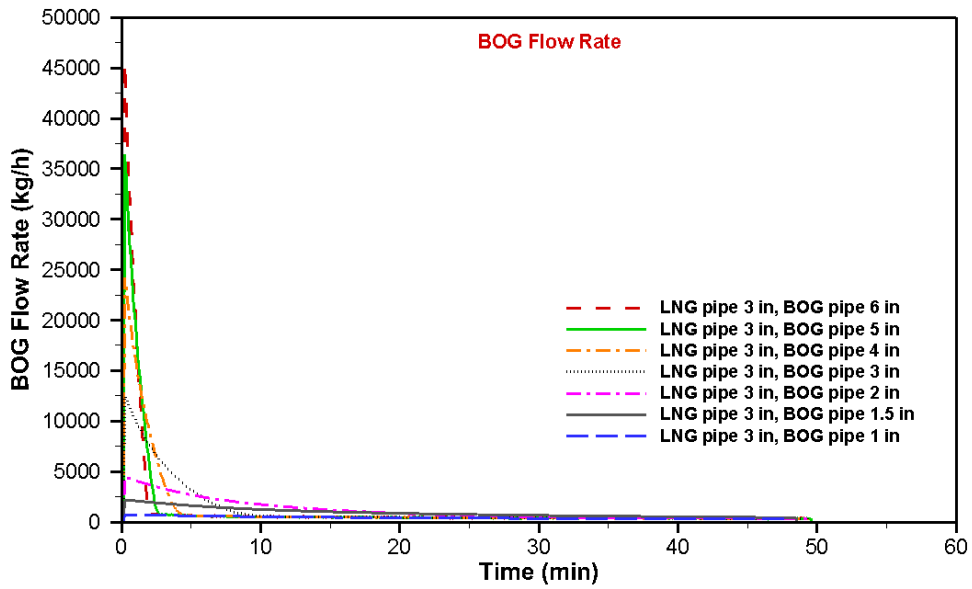
(Comparison of TTS and STS Bunkering Case)

According to the current LNG bunkering situation, there is no uniform standard for the diameter of LNG pipelines and BOG pipelines. The diameter ratio of the pipeline is also one of the main factors affecting the LNG bunkering. Therefore, the LNG bunkering process was optimized by different dynamics simulation studies focus on the amount of BOG return and pump head. This section compares the TTS and STS filling methods.

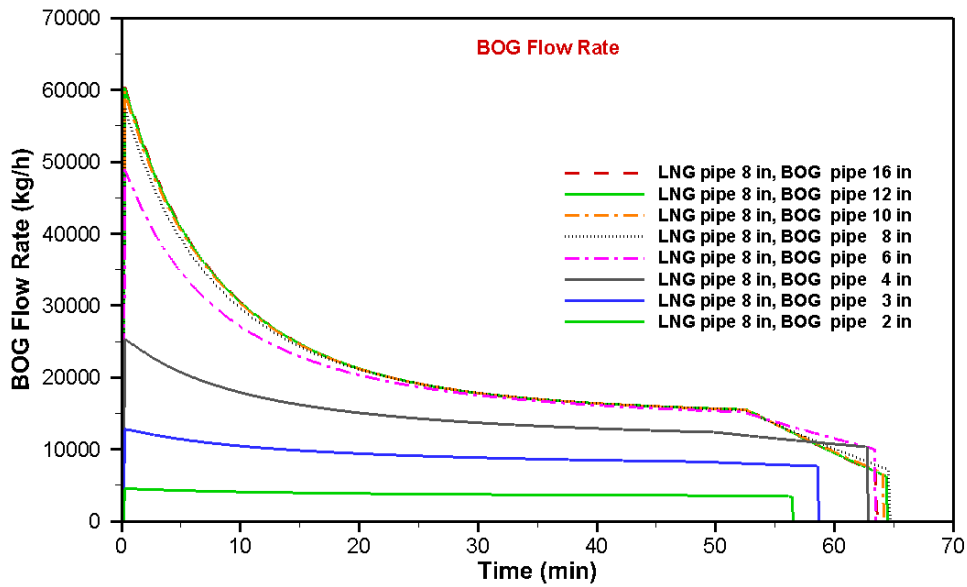
1) Transient BOG variation

Fig. 4.19 shows the variation of the BOG flowrate in the receiving tank in different diameter of BOG return pipeline (DB). Both in the TTS and STS LNG bunkering cases, the initial BOG flowrate is proportional to the DB. This is because at the beginning of the bunkering process, when the pump was started, a large amount of heat entering the LNG was transferred from the bunkering ship (tank truck) to the receiving ship. Consequently, the bigger the DB the more BOG generation transfer to the bunkering ship or LNG tank truck. This point is more obvious in TTS bunkering case. The maximum BOG flowrate reaches more 4,500 kg/h when the DB is 6 in.

As shown in the figures, with the receiving ship filling up, the BOG flow rate decreases in all cases. Furthermore, the BOG generation was gradually reduced in the TTS case. At the end of the bunkering process, as the LNG is no longer transported to the receiving ship, the BOG flow rate dropped rapidly as the pump shutdown. In addition, the total bunkering time was proportional to the DB due to the bigger the DB, the more BOG flowed through the BOG pipe to the bunkering facilities.



(a) TTS LNG bunkering method



(b) STS LNG bunkering method

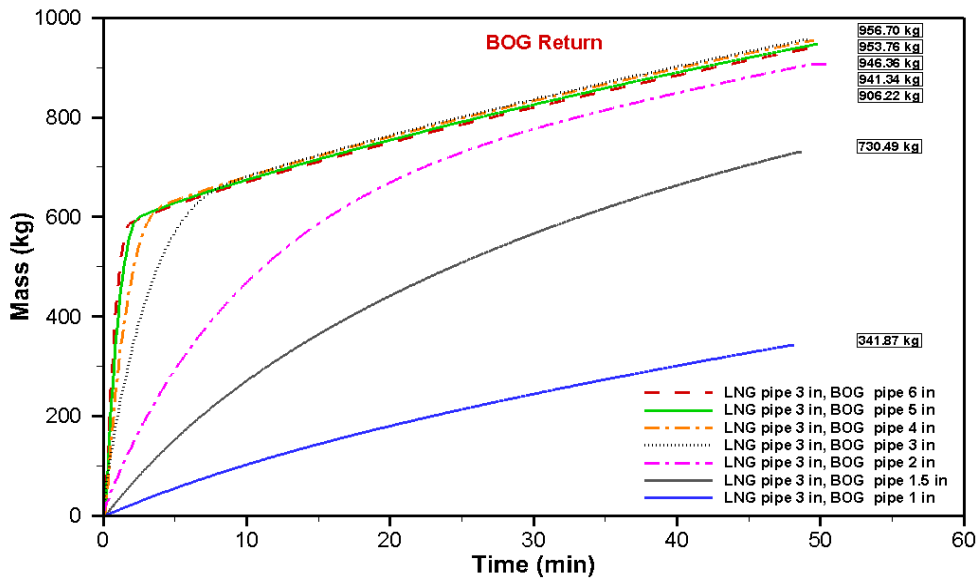
Fig. 4.19 BOG flow rate variation based on different diameter of BOG pipeline.

2) BOG return

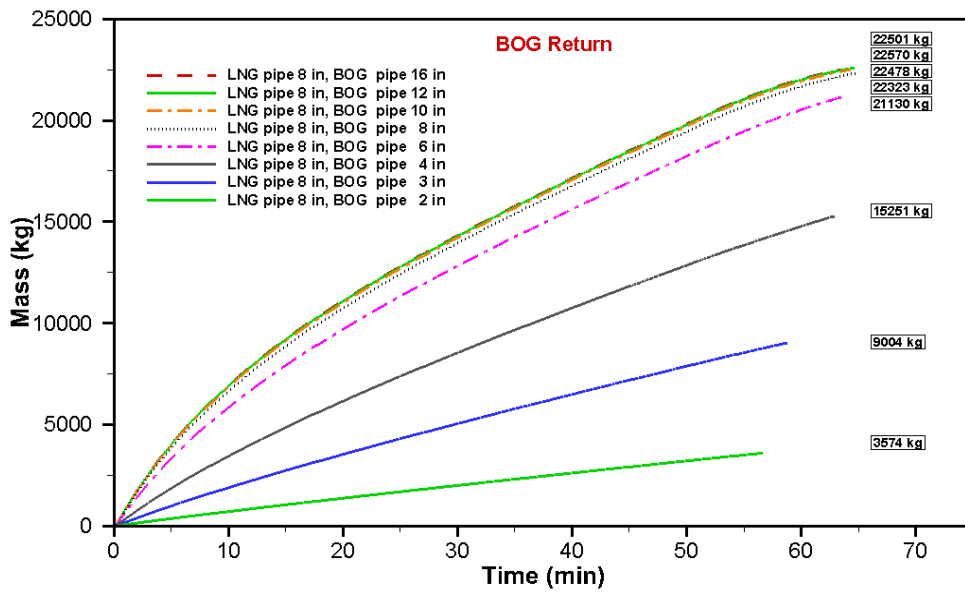
Fig. 4.20 shows the variation of the BOG return in the receiving tank in different diameter of BOG return pipeline (DB). As can be seen from the figures, both the TTS and STS bunkering Case, the amount of BOG return from receiving ship (tank truck) is increasing rapidly and proportionally with the DB increasing in each case. This point is significantly expressed in the TTS bunker case, especially when the diameter ratio of the BOG and LNG pipeline over 1 ($DB/DL > 1$). This is because the temperature difference between the tank truck and the receiving ship become closed rapidly. It could be confirmed in the next section. Additionally, the mass of BOG return is almost same when the $DB/DL > 1$ in all the cases. It can be expressed as no matter how much the diameter of the BOG pipeline is increased, the BOG amount hardly changes. Conversely, as the diameter of the BOG pipeline decreases, the total amount of BOG decreases, proportionally.

3) Variations in the bunker and receiver tank pressure

Fig. 4.21 shows that, both the TTS and STS bunkering method, the pressure difference between the bunkering ship (tank truck) and receiving ship is close to each other with the bunkering process. This point is significantly expressed in the TTS bunkering case due to the two tanks' capacity is similar. For the STS bunkering method, the amount of BOG generation decreases due to the increasing of LNG bunkering. When the tank level of receiving ship reached at 85%, the pressure rate in bunkering ship is increased due to decreased of LNG flowrate, which could be seen in Fig. 4.21 (b).

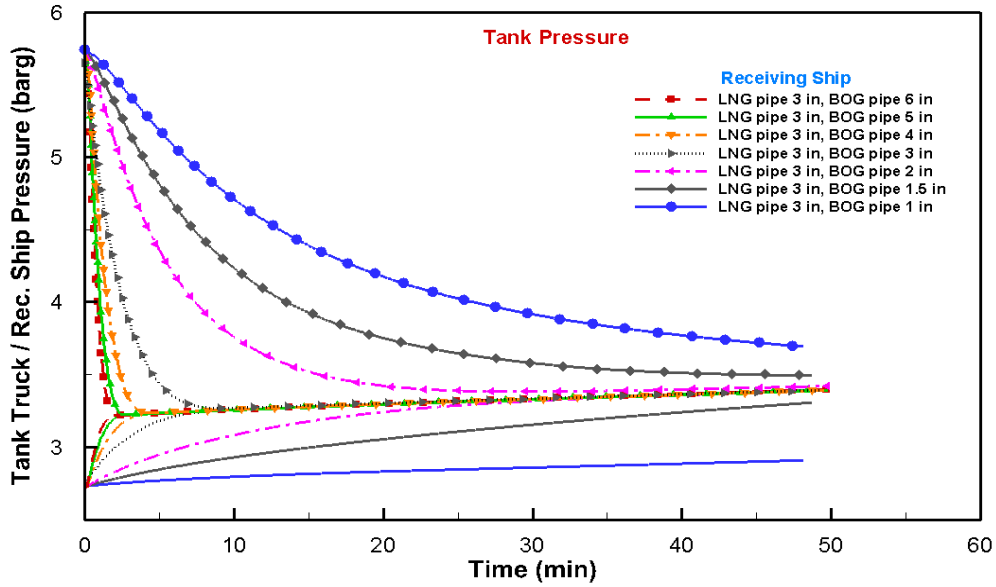


(a) TTS LNG bunkering method

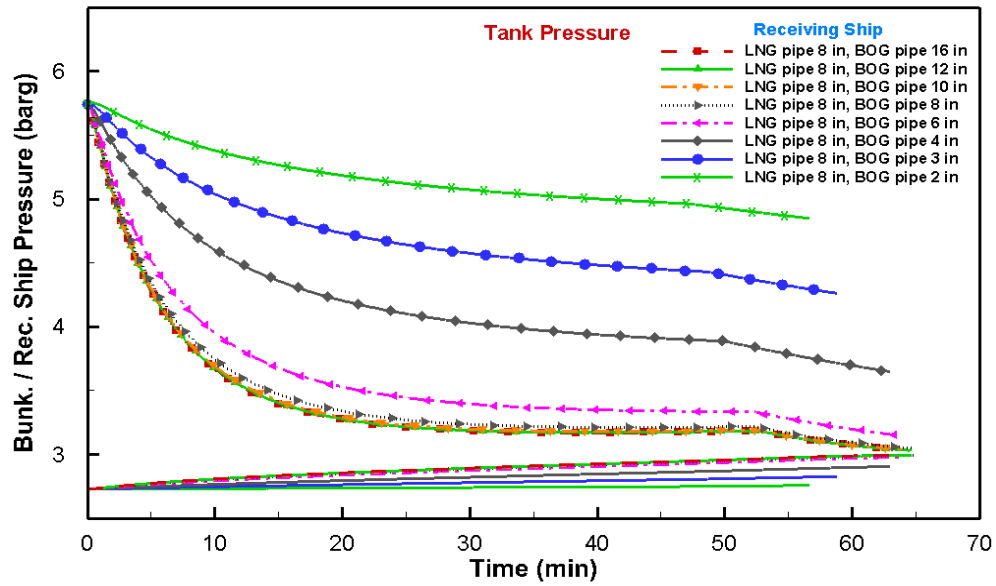


(b) STS LNG bunkering method

Fig. 4.20 BOG profile during bunkering operation for the BOG from the receiving tank at different diameter of BOG pipeline.



(a) TTS LNG bunkering method



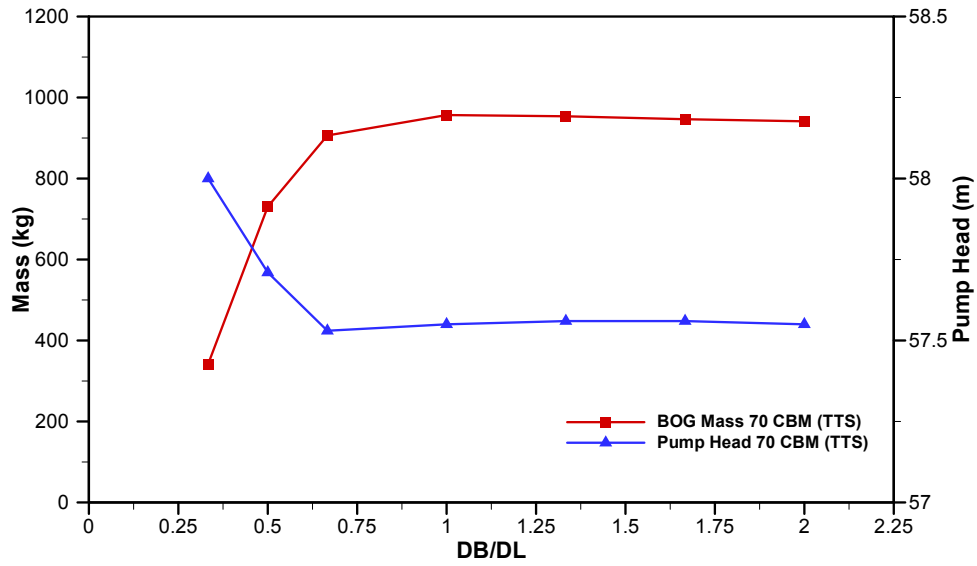
(b) STS LNG bunkering method

Fig. 4.21 Pressure variation in the bunker and receiving ship during the bunkering operation at different diameter of BOG pipeline.

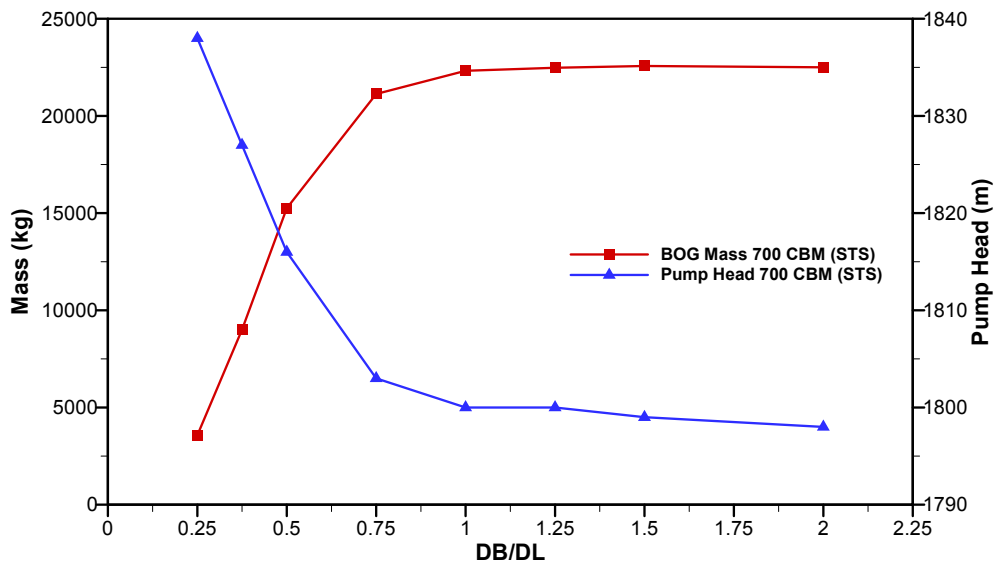
4) Optimization for the diameter ratio of BOG and LNG pipeline

Since the LNG-fueled ship was commercialized after the 21st century, and the bunkering infrastructure facilities lacked design and operating experience. Therefore, there was a few appropriate industry standards for the LNG bunkering process. This section, dynamic simulation was carried out to examine the different diameter ratio of BOG and LNG pipeline during TTS and STS LNG bunkering, optimized the diameter ratio by the amount of BOG mass and pump head factors. The simulation results could be helpful as a feasibility study and provide the theoretical reference for the operating standards of the LNG bunkering process.

Fig. 4.22 shows the amount of BOG mass and pump head changes during the bunkering operation at the different diameter ratio of BOG and LNG pipeline. Both in the TTS and STS bunkering method, the variation of BOG amount was increasing until the $DB/DL = 1$, when the $DB/DL > 1$ the amount of BOG mass little changed. It can be expressed as no matter how much the diameter of the BOG pipeline is increased, the BOG amount hardly changes. On the contrary, for the variation of pump head, it was continuous decreasing until the $DB/DL = 1$ both in the TTS and STS bunkering method. For the STS LNG case the pump head decreased gradually when the DB/DL is from 1 to 2. Therefore, in order to find the optimal diameter ratio during the LNG bunkering process, when $DB/DL > 1$, it was obviously not appropriate because a large amount of BOG was generated. Similarly, when the $DB/DL < 0.5$, it produced the lowest amount of BOG, but the pump head was the highest and will consume more energy. So, when the $DB/DL = 0.5$ is considered to be the best.



(a) TTS LNG bunkering method



(b) STS LNG bunkering method

Fig. 4.22 BOG mass and pump head during the bunkering operation at different diameter ratio of BOG and LNG pipeline.

Chapter 5 Conclusions

The study focused on the changes in the BOG generation and other effects of ship-to-ship (STS) and truck-to-ship (TTS) LNG bunkering procedures given in the different conditions. Based on the dynamic simulation, an optimal LNG bunkering time limit and an optimal ratio of pipeline diameter were proposed. In addition, a formula for calculating BOG amount which can substitute for simulation is established. The results in different bunkering scenarios were obtained as follows:

(1) The boil-off rate and consequent pressure buildup in the receiving vessel were mainly determined by the temperature difference between the bunkering and receiving tanks, the pressure of the receiver tank, and the amount of remaining LNG.

(2) The amount of BOG generation and BOG returns were proportional to the temperature difference between the bunkering and receiving tanks.

(3) As the quantity of the BOG increased the pressure in the receiving fuel tank increased as well, and the variation of transient pressure for both tanks was proportional to the temperature difference.

(4) In addition to the temperature difference, the BOG generation is also related to the MN. The amount of BOG generation from receiving ship is proportional with the MN.

(5) Although there is a certain relationship between the BOG generation and MN, it is not the critical factor compared with the temperature difference for the entire LNG bunkering process. The gap between the maximum mass

of BOG and the minimum mass of BOG was less than 4%.

(6) With the respect of the optimal bunkering time limit, in the initial 20 min. of all the bunkering cases, the BOG flow rate was directly proportional to the bunkering time limit. Conversely, the BOG flow rate was inversely proportional to the bunkering time limit after 20 min.

(7) The bunkering time should be controlled within 120 min. to avoid the generation of additional BOG when the capacity of the pump exceeded 100,000 kg/h. Conversely, when the pump's capacity was lower than 100,000 kg/h, the bunkering efficiency could be improved properly to reach the optimal time limit.

(8) The tank pressure difference between bunkering and receiving ship reduced with increases in the bunkering time limit. Additionally, when the level of fuel tank for the receiving ship reached 85%, the pressure in the bunker tank increased due to decreases in the LNG flow rate.

(9) With the respect of the optimal ratio for the pipeline diameter, when the $DB/DL = 0.5$ is considered the best value both in the STS and TTS LNG bunkering methods, thus the tank pressure difference between bunkering and receiving ship may be reduced.

Several challenges were identified for the future studies. The present study only provides a mathematical model for the calculation of the total amount of BOG generation by the STS LNG bunkering method, while the current LNG bunkering methods also include the Truck-to-ship (TTS) and Pipe-to-ship (PTS). In order to develop the general BOG equation, a number of LNG bunkering scenarios in different conditions need to be examined. What's more, the further research should attach importance to the impacts of the

environmental conditions in the surrounding bunkering area to the BOG generation. The factors such as sea stability, atmospheric temperature and other conditions will be included to enhance the reliability of data.

Additionally, the limitation of the present study was that the object fuel tank for the receiving ship is the IMO type C pressure tank which commonly used in the current LNG fueled ships. The bunkering conditions for large container ships with the possibility of using the membrane tanks in the future were not considered. Although this study had some limitation, considering that the lack of industry practices and standards in determining the LNG bunkering time limit and the mass of BOG generation calculations, it is believed that the insights present in this paper could provide useful information as a complement.

References

- ABS, 2014. *LNG bunkering: Technical and Operational Advisory*, American Bureau of Shipping Press: Houston.
- Adachi, M., Kosaka, H., Fukuda, T., Ohashi, S. & Harumi, K., 2014. Economic analysis of trans-ocean LNG-fueled container ship. *Journal of Marine Science and Technology*, 19, pp. 470-478.
- Andersen, M., Clausen, N. & Sames, P., 2011. *Costs and benefits of LNG as ship fuel for container vessels*. Ger.Lloyd & MAN.
- Aspen Technology, 2017. *HYSYS Operations Guide*, V10, Aspen Technology Inc.: Burlington, MA, USA.
- Aymelek, M., Boulougouris, E.K., Turan, O. & Konovessis, D., 2014. Challenges and opportunities for LNG as a ship fuel source and an application to bunkering network optimisation. *Proceedings of International Conference on Maritime Technology and Engineering*; Oct 15-17; Lisbon, Portugal. London: Taylor & Francis Group, pp. 767-776.
- Bahgat, W.M., 2015. Proposed method for dealing with boil-off gas on board LNG carriers during loaded passage. *International Journal of Multidisciplinary and Current Research*, 3, pp. 508-512.
- Van den Beemt, B., Van Bokhorst, E., Van der Weijde, G., Mallon, N. & Verweij, S., 2009. Qualification of LNG STS Transfer Flexibles According to Guideline EN1474-II, *Offshore Technology Conference (OTC)*, Houston, Texas, USA.
- BS EN 1474-2:2008, 2008. *Installation and Equipment for Liquefied Natural Gas, Design and Testing of Marine Transfer Systems Design and Testing*

- of Transfer Hoses*. British Standards.
- Carolina R., 2017. LNG Bunkering. *Congreso GASNAM El Gas Natural Garantiza la Calidad del Aire*, Madrid, 8th March.
- Chun, J.M., Kang, H.K., Kim, Y.T., Jung, M.H. & Cho, K.H., 2016. Case study on operating characteristics of gas fueled ship under the conditions of load variation, *Journal of Korean Society of Marine Engineering*, 40(5), pp. 447-452.
- Dale H.B. & James P.B., 1973. A study of two-phase flow in inclined pipes, *J. Petrol. Technol.* 25(05), pp. 607-617.
- Dobrata, D., Lalic, B. & Komar, I., 2013, Problem of Boil-off in LNG Supply Chain, *Journal of Transactions On Maritime Science*, No. 2, pp. 91-100.
- DMA, 2012. *North European LNG Infrastructure Project - A feasibility study for an LNG filling station infrastructure and test of recommendations*. Danish Maritime Authority.
- DNV GL Rules, 2015. *Development and operation of liquefied natural gas bunkering facilities*, DNV·GL.
- Effendy, S., Khan, M.S., Farooq, S. & Karimi, I.A., 2017. Dynamic modelling and optimization of an LNG storage tank in a regasification terminal with semi-analytical solutions for N₂-free LNG. *Computers & Chemical Engineering*, 99, pp. 40-50.
- EMSA, 2018. *Guidance on LNG Bunkering to Port Authorities and Administration*. European Maritime Safety Agency (EMSA) Press: Lisbon.
- Fan, H., Cheng, K. & Wu, S., 2017. CFD based simulation of LNG release

- during bunkering and cargo loading/unloading simultaneous operations of a containership. *Journal of Shipping and Ocean Engineering*, 7, pp. 51-58.
- Fluxys LNG, 2012. *Safety Study, Chain analysis : Supplying Flemish ports with LNG as a marine fuel*, M-tech protec Engineering.
- GL, 2013. *European Maritime Safety Agency (EMSA) - Study on Standards and Rules for bunkering of gas-fuelled Ships*. Version 1.1, Germanischer Lloyd.
- Ha, S. M., Lee, W. J., Jeong, B., Choi, J. H. & Kang, J., 2019. Regulatory gaps between LNG carriers and LNG fuelled ships. *Journal of Marine Science and Technology*, 4177, pp. 1-15.
- Harperscheidt, J., 2011. *LNG Storage and Fuel Gas Systems*, LNG: Fuel for Shipping, London.
- Hasan, M.M.F., Zheng, A.M. & Karimi, I.A., 2009. Minimizing boil-off losses in liquefied natural gas transportation. *Industrial & Engineering Chemistry Research*, 48, pp. 9571-9580.
- IEO, 2011. *International Energy Outlook 2011*. U.S. Energy Information Administration press.
- IGU, 2018. *2018 World LNG Report (2018 Edition)*. Barcelona: International Gas Union.
- Ikealumba, W.C. & Wu, H., 2014. Some Recent Advances in Liquefied Natural Gas (LNG) Production, Spill, Dispersion, and Safety. *Energy & Fuels*, 28(6), 3556-3586.
- IMO, 2003. *International Code for the Construction and Equipment of Ships Carrying Liquefied Gas in Bulk*. International Maritime Organization

(IMO): London, UK.

IMO, Sulphur Oxides (SO_x) and Particulate Matter (PM), Available online: [http://www.imo.org/en/OurWork/Environment/PollutionPrevention/AirPollution/Pages/Sulphur-oxides-\(SO_x\)-%E2%80%93-Regulation-14.aspx](http://www.imo.org/en/OurWork/Environment/PollutionPrevention/AirPollution/Pages/Sulphur-oxides-(SO_x)-%E2%80%93-Regulation-14.aspx) (accessed on 20 April 2018).

ISO, 2015. *ISO/TS 18683:2015 Guidelines for systems and installations for supply of LNG as fuel to ships*. ISO.

ISO 20519:2017, 2017. *Ships and marine technology – Specification for bunkering of liquefied natural gas fueled vessels*. 1st ed., ISO: Geneva, Switzerland.

Jeong, B., 2018. *On The Safety Of LNG-Fuelled Ship*. Ph.D. Dissertation, Department of Naval Architecture, Ocean and Marine Engineering, University of Strathclyde.

Jeong, B., Lee, B.S., Zhou, P. & Ha, S., 2017. Evaluation of safety exclusion zone for LNG bunkering station on LNG-fuelled ships. *Journal of Marine Engineering & Technology*, 4177, pp. 1–24.

Kumar R., 2006. *Aspen simulation liquefied natural gas import terminal safety and security study*. Master Thesis, Lamar University.

Kurle, Y.M., Wang, S. & Xu, Q., 2015. Simulation study on boil-off gas minimization and recovery strategies at LNG exporting terminals. *Applied Energy*, 156, pp. 628–641.

Kurle, Y.M., Wang, S. & Xu, Q., 2017. Dynamic simulation of LNG loading, BOG generation, and BOG recovery at LNG exporting terminals. *Computers & Chemical Engineering*, 97, pp. 47–58.

Kurle, Y.M., Xu, Q. & Palanki, S., 2018. Dynamic Simulation Study for

- Boil-off Gas Minimization at Liquefied Natural Gas Exporting Terminals. *Industrial & Engineering Chemistry Research*, 57(17), pp. 5903–5913.
- Lee, J., Ryu, J. & Chung, H., 2016. Liquefied natural gas ship-to-ship bunkering chain planning : Case studies of Busan, Singapore, and Rotterdam ports. *Proceedings of the Institution of Mechanical Engineers, Part M: Journal of Engineering for the Maritime Environment*, 231(2), pp. 1-10.
- Lee, M.H., Shao, Y.D., Kim, Y.T. & Kang, H.K. (2017), Performance characteristics under various load conditions of coastal ship with LNG-powered system, *Journal of Korean Society of Marine Engineering*, 41(5), pp. 424-430.
- Lee, S., Jeon, J., Lee, U. & Lee, C., 2015. A Novel Dynamic Modeling Methodology for Boil-Off Gas Recondensers in Liquefied Natural Gas Terminals. *Journal of Chemical Engineering of Japan*, 2015, 48, 841–847.
- Lee, S., Seo, S. & Chang, D., 2015. Fire risk comparison of fuel gas supply systems for LNG fuelled ships. *Journal of Natural Gas Science and Engineering*, 27, pp. 1788–1795.
- Li, Y. J. & Chen, X. S., 2012. Dynamic Simulation for Improving the Performance of Boil-Off Gas Recondensation System at LNG Receiving Terminals. *Chemical Engineering Communications*, 10, pp. 1251-1262.
- MAN, 2009. *Propulsion Trends in LNG Carriers*, MAN Diesel & Turbo: Copenhagen, Denmark.
- Miana, M., Hoyo, R. & Rodrigalvarez, V., 2016 Comparison of Evaporation Rate and Heat Flow Models for Prediction of Liquefied Natural Gas (LNG) Ageing during Ship Transportation. *Fuel*, 177, pp. 87–106.

- Michelsen F.A., Halvorsen I.J., Lund B.F., et al., 2010. Modeling and simulation for control of the TEALARC liquefied natural gas process. *Industrial & Engineering Chemistry Research*, 49(16), pp. 7389-7397.
- Migliore, C., Tubilleja, C. & Vesovic, V., 2015. Weathering prediction model for stored liquefied natural gas (LNG). *Journal of Natural Gas Science and Engineering*, 26, pp. 570-580.
- MOTIE, 2017. *Promising New Industry Standardization Roadmap*, Korea Institute for Advancement of Technology.
- Nguyen, L., Kim, M. & Choi, B., 2017. An experimental investigation of the evaporation of cryogenic-liquid- pool spreading on concrete ground. *Applied Thermal Engineering*, 123, pp. 196-204.
- Notteboom, T., 2011. The impact of low sulphur fuel requirements in shipping on the competitiveness of ro-ro shipping in Northern Europe. *WMU Journal of Maritime Affairs*, 10, pp. 63-95.
- Park, C., Cho, B., Lee, S. & Kwon, Y., 2016. Study on the Re-liquefaction Processing for Boil off Gas System of Floating Offshore LNG Bunkering Terminal. *Proceedings of the Twenty-sixth International Ocean and Polar Engineering Conference*, Rodes, Greece, 26 June - 1 July, International Society of Offshore and Polar Engineers (ISOPE), Mountain View, CA, USA.
- Park, C., Song, K., Lee, S., Lim, Y. & Han, C., 2012 Retrofit design of a boil-off gas handling process in liquefied natural gas receiving terminals. *Energy*, 44, pp. 69-78.
- Peebles, M.W.H., 1992. *Natural Gas Fundamentals*, Shell International Gas Limited: The Hague, Netherlands.

- PGS, 2013. *Natural gas – liquefied natural gas (LNG) delivery installations for vehicles*. Hazardous Substances Publication Series 33-1: 2013 version 1.0, Publicatiereeks Gevaarlijke Stoffen (PGS).
- Rao, H.N., Karimi, I.A. & Farooq, S., 2018. Optimal Design of Boil-Off Gas Liquefaction in LNG Regasification Terminals. *Computer Aided Chemical Engineering*, 44, pp. 2407-2412.
- Ravenswaay, J.P., Greyvenstein, G.P., Neikerk, W.M.K. & Labuschagne, J.T., 2006. Verification and validation of the HTGR systems CFD code Flownex. *Nuclear Engineering and Design*, 236, pp. 491–501.
- Rudan, S., Ascic, B. & Visic, I., 2013. *Proceedings of the 6th International Conference on Collision and Grounding of Ship and Offshore Structures*; Trondheim, Norway, 17–19 June, pp 331–337.
- Ryu, J.H., 2012. *Concept for protection against overpressure caused by BOG generated during ship-to-ship LNG bunkering*, Master Thesis, Department of Ocean Systems Engineering, Korea Advanced Institute of Science and Technology (KAIST).
- Seo, Y., Lee, S., Kim, J., Huh, C. & Chang, D., 2017. Determination of optimal volume of temporary storage tanks in a ship-based carbon capture and storage (CCS) chain using life cycle cost (LCC) including unavailability cost. *International Journal of Greenhouse Gas Control*, 64, pp. 11–22.
- Shao, Y.D., Kang, H.K., Yoon, S.D. & Kim Y.T., 2017. Dynamic Simulation for Boil-off Gas in LNG Fueled Ship during Ship-to-ship Bunkering Process. *Proceedings of the International Symposium on Marine Engineering (ISME)*, Tokyo, 15-19 October, Japan Institute of Marine

- Engineering (JIME): Tokyo, Japan.
- Shao, Y.D., Lee, Y.H., Kim, Y.T. & Kang, H.K., 2018. Parametric Investigation of BOG Generation for Ship-to-Ship LNG Bunkering. *Journal of the Korean Society of Marine Environment & Safety*, 3, pp. 352-359.
- Sharafian, A., Herrera, O.E. & Merida, W., 2016. Performance Analysis of Liquefied Natural Gas Storage Tanks in Refueling Stations. *Journal of Natural Gas Science and Engineering*, 36, pp. 496–509
- Shariq, M., Effendy, S., Karimi, I.A. & Wazwaz, A., 2019. Improving design and operation at LNG regasification terminals through a corrected storage tank model. *Applied Thermal Engineering*, 149, pp. 344-353.
- Silva, L.D.S. & Marinho, J.L.G., 2016. Study on Pressure Drop and Liquid Volume Fraction of the Oil-Gas Flow in a Vertical Pipe Using CFX and the Beggs and Brill Correlation: Viscosity Effects. *Brazilian Journal of Petroleum and Gas*, 10 (1), pp. 1-8.
- SMTF, 2010. *LNG bunkering Ship to Ship procedure*, Swedish Marine Technology Forum.
- Soave, G., 1972. Equilibrium constants from a modified Redlich-Kwong equation of state. *Chemical Engineering Science*, 6, pp. 1197-1203.
- Stryjek, R. & Vera, J.H., 1986. PRSV: An Improved Peng- Robinson Equation of State for Pure Compounds and Mixtures. *The Canadian Journal of Chemical Engineering*, 64, pp. 323-333.
- Sun, B., Guo, K. & Pareek, V.K., 2017. Hazardous consequence dynamic simulation of LNG spill on water for ship-to-ship bunkering. *Process Safety and Environmental Protection*, 107, pp. 402-413.

- Wang, S.Y. & Notteboom, T., 2014. The Adoption of Liquefied Natural Gas as a Ship Fuel: A Systematic Review of Perspectives and Challenges. *Transport Reviews*, 34, pp. 749-774.
- Wang, S. & Notteboom T., 2015. The role of port authorities in the development of LNG bunkering facilities in North European ports. *WMU Journal of Maritime Affairs*, 14, pp. 61-92.
- Wang Y., Shen J., Wang Q., Wu D. & Jin C., 2018. Evaluation Technology of Design Scheme for Liquefied Natural Gas Bunker Vessel, *Journal of Shanghai Jiaotong University (Science)*, 52(6), pp. 693-697.
- Wärtsilä, Methane Number Calculator, [Online] Available at: <https://www.wartsila.com/products/marine-oil-gas/gas-solutions/methane-number-calculator> (accessed on 15 August 2018).
- Westerberg, A.W., Hutchison, H.P., Motard, R.L. & Winter, P., 1979. *Process Flowsheeting*. Cambridge University Press: Cambridge.
- Woehrling, J.M. & Cotterell, C.D., 2010. *International Safety Guide for Inland Navigation Tank-barges and Terminals (ISGINTT)*, Central Commission for the Navigation of the Rhine: Strasbourg, France.
- Wu, M., Zhu, Z., Sun, D., He, J., Hu, B. & Tian, S., 2019. Optimization model and application for the recondensation process of boil-off gas in a liquefied natural gas receiving terminal. *Applied Thermal Engineering*, 147, pp. 610-622.
- Xu, J.Y., Fan, H.J., Wu, S.P. & Shi, G.Z., 2015. Research on LNG Ship to Ship (STS) Bunkering Operations, *Journal of Ship Engineering*, 37(1), pp. 7-10.
- Xu, J., Testa, D. & Mukherjee, P.K., 2015. The Use of LNG as a Marine

- Fuel: The International Regulatory Framework. *Ocean Development & International Law*, 46, pp. 225-240.
- Yan, G. & Gu, Y., 2010. Effect of parameters on performance of LNG-FPSO offloading system in offshore associated gas fields. *Applied Energy*, 87, pp. 3393-3400.
- Yun, S., Ryu, J., Seo, S., Lee, S., Chung, H., Seo, Y. & Chang D., 2015. Conceptual design of an offshore LNG bunkering terminal: a case study of Busan Port. *Journal of Marine Science and Technology* 2, pp. 226-237.
- Zakaria, M., Osman, K., Yusof A., Hanafi, H., Saadun, M. & Manaf, M., 2014. Parametric analysis on boil-off gas rate inside liquefied natural gas storage tank. *Journal of Mechanical Engineering and Sciences (JMES)*, 6, pp. 845-853.